

A study on fault diagnosis in nonlinear dynamic systems with uncertainties

Steven X. Ding

Institute for Automatic Control and Complex Systems (AKS)
University of Duisburg-Essen, 47057 Duisburg, Germany

Linlin Li

School of Automation and Electrical Engineering
University of Science and Technology Beijing, Beijing 100083, China

Abstract: In this draft, fault diagnosis in nonlinear dynamic systems is addressed. The objective of this work is to establish a framework, in which not only model-based but also data-driven and machine learning based fault diagnosis strategies can be uniformly handled. To this end, a paradigm is followed, which is different from the control theoretically oriented model-based framework. Instead of the well-established input-output and the associated state space models, stable image and kernel representations are adopted in our work as the basic process model forms. The idea behind this handling is to deal with fault diagnosis issues in the process input-output data space, along the line of data-driven and machine learning methods. Using the image and kernel representations the nominal system dynamics can then be modelled as a lower-dimensional manifold embedded in the process data space. To achieve a reliable fault detection as a classification problem, projection technique is a capable tool that projects the process data onto the image manifold towards classifying the nominal dynamics and faulty/uncertain dynamics. For nonlinear dynamic systems, we propose to construct projection systems in the well-established framework of Hamiltonian systems and by means of the normalised image and kernel representations. It is known that, in case of linear systems, the norm-based evaluation of the residual signal, created from the difference between the data and its projection, is widely used in fault detection. Thanks to the Hilbert Projection Theorem and the Pythagorean equation, the norm-based evaluation can uniquely distinguish nominal dynamics from the faulty/uncertain dynamics. For nonlinear dynamic systems, process data form a non-Euclidean space. Consequently, the norm-based distance defined in Hilbert space is not suitable to measure the distance from a data vector to the manifold of the nominal dynamics. To deal with this issue, we propose to use a Bregman divergence, a measure of difference between two points in a space, as a solution. Moreover, for our purpose of achieving a performance-oriented fault detection, the Bregman divergences adopted in our work are defined by Hamiltonian functions. A distinguishing contribution of our work is the development of a scheme that combines the Hamiltonian systems, their Legendre dual systems and Bregman divergences induced by the corresponding Hamiltonian functions. This scheme not only enables to realise the performance-oriented fault detection, but also uncovers the information geometric aspect of

our work. Specifically, the Bregman divergence together with Hamiltonian Legendre dual systems may induce a dually flat Riemannian manifold in the data space that is regarded as a dualistic extension of the Euclidean space. In this context, the Hamiltonian system based projection can be interpreted as a geodesic projection. The last part of our work is devoted to the kernel representation based fault detection and uncertainty estimation that can be equivalently used for fault estimation. To this end, the concepts of the uncertainty model and the manifold of uncertainty data are introduced and used to model uncertainties (including faults) corrupted in the process data. It is demonstrated that the projection onto the manifold of uncertainty data, together with the correspondingly defined Bregman divergence, is also capable for fault detection. In particular, it is proved that such a projection is a least squares estimation of the uncertainty corrupted in data and subject to the uncertainty model. Hence, the kernel representation based projection can serve as an optimal estimator for variations in the process data caused by faults.

Keywords: Fault detection and estimation, projection- and observer-based fault detection and estimation, Hamiltonian systems, Bregman divergences, Legendre transform, information geometry, uncertainty and uncertainty model

1 Introduction

Having undergone a rapid development over a couple of decades, model-, in particular, observer-based fault diagnosis technique has become well established as an active research area in control theory and engineering (Frank, 1990; Frank and Ding, 1997; Venkatasubramanian *et al.*, 2003; Mangoubi *et al.*, 2009; Hwang *et al.*, 2010; Gao *et al.*, 2015; Zhong *et al.*, 2018). Technically speaking, an observer-based fault detection system consists of two major units, a residual generator and evaluator. For their design and analysis system input-output and the associated state space models build a common basis, and advanced control theoretical methods serve as the major theoretical tool (Patton *et al.*, 1989; Gertler, 1998; Chen and Patton, 1999; Blanke *et al.*, 2006; Ding, 2008). Specifically, the observer-based residual generator design is mainly achieved by means of advanced observer theory, while the construction of the evaluator with a focus on the threshold setting is performed on the basis of norm-based system analysis (Ding, 2008; Ding, 2020). To put it in a nutshell, state of the art of observer-based fault diagnosis technique is marked by the well-established framework for fault diagnosis in linear time invariant (LTI) systems, while a systematic dealing with fault diagnosis issues is missing for nonlinear systems.

In their survey (Alcorta-Garcia and Frank, 1997), Alcorta-Garcia and Frank reviewed state of the art of nonlinear observer-based fault detection in the 90's. The major methods include the application of feedback-based linearisation and differential algebra techniques to observer-based residual generator design (Seliger and Frank, 1991; Hammouri *et al.*, 1999; Kabore and Wang, 2001), and the geometric approach to nonlinear fault detection (Persis and Isidori, 2001). Later, considerable attention has been paid to the application of those special techniques that enable dealing with analysis and synthesis of nonlinear dynamic systems more efficiently. These are, amongst others, linear matrix inequalities (LMI) technique to address a special class of nonlinear systems with, for instance, Lipschitz nonlinearity (Pertew *et al.*, 2007; Zhang *et al.*, 2010b) or sector bounded nonlinearity (He *et al.*, 2009), fuzzy technique based fault detection (Nguang *et al.*, 2007; Chadli *et al.*, 2013; Shen *et*

al., 2014; Li *et al.*, 2016; Li *et al.*, 2017), adaptive fault diagnosis for nonlinear systems (Xu and Zhang, 2004; Zhang *et al.*, 2010a; Shen *et al.*, 2014), linear parameter-varying fault detection systems (Bokor and Balas, 2004; Armeni *et al.*, 2009), and sliding mode observer-based fault detection (Floquet *et al.*, 2004; Yan and Edwards, 2008). Although all these efforts are successful in dealing with fault detection of the corresponding system classes, a common theoretical framework for design and analysis of nonlinear fault detection systems seems missing. In our early efforts towards such a framework, we noticed that little attention was paid to essential issues of nonlinear observer-based fault detection systems like existence conditions, detectability and parameterisation. With the aid of nonlinear system theory as a major tool (Vidyasagar, 1980; Sontag and Wang, 1995; Lu, 1995; van der Schaft, 2000), these issues have been examined and the first results were reported in (Yang *et al.*, 2015; Yang *et al.*, 2016; Ding, 2020).

Fault detection is a classification problem, namely classifying those potential anomalies from the collected data during system operations. The use of a system model and, based on it, an observer allows to distinguish anomalies from the normal input-output dynamics and thus leads to an efficient classification. On the other hand, in industrial practice, the use of a mathematical model is generally associated with model uncertainties. Coupled with external disturbances (unknown inputs), they considerably complicate a reliable classification, in particular when nonlinear dynamic systems are under consideration. In fact, distinguishing anomalies/faults from the uncertainties existing during fault-free operations is a most crucial issue in dealing with classification/fault detection. A further challenging issue is to detect process faults, also called component faults in the literature (Frank, 1990; Ding, 2008). As reported in innumerable publications, observer-based fault detection methods are capable to detect sensor and actuator faults in dynamic systems. Two plausible reasons for such successful applications are, (i) an input-output model gives a natural modelling of sensor and actuator faults, (ii) the norm-based evaluation of residual signals (the difference of the measurement and its estimate) builds an explicit indicator for these two types of faults. Differently, process faults are corrupted with model uncertainties, and as a consequence of nonlinear system dynamics, process data build a manifold that is a non-Euclidean space. It is known that usual Euclidean distances or inner products may not be appropriate to measure the dissimilarity between the data points on a manifold, which is the core purpose of classification. That process faults as well as uncertainties can result in remarkable system performance degradation, but are hardly detected using norm-based evaluation function is the further aspects that motivate our work.

In the era of artificial intelligence and big data, machine learning (ML) based classification methods have become for a long time now the mainstream in the research area of engineering fault diagnosis. Classification-based fault diagnosis is a technique that uses ML-classifiers to detect faults in a system based on the features extracted from the process data. As a crucial step towards reliable and explainable fault diagnosis, dimensionality reduction technique, also known as manifold learning, serves as a capable tool, where the irrelevant and redundant informations in the data are reduced, leading to not only lower computation complexity but also, and more importantly, better classification and fault diagnosis performance. In order to capture nonlinear and nonstationary characteristics of the data, nonlinear dimensionality reduction methods have been developed, among them, the so-called Isomap (Isometric mapping) (Tenenbaum *et al.*, 2000) and LLE (Locally-linear embedding) (Roweis and Saul, 2000) are two representative ones. Informally speaking, an essential assumption

in manifold learning is that the data have been generated from a lower-dimensional manifold that is embedded inside of a higher-dimensional space composed of redundant and irrelevant information (uncertainties). The basic idea of Isomap is the use of a geodesic distance, which enables to incorporate the manifold structure in the resulting embedding. The objective of the LLE algorithm is to create a data mapping from the higher-dimensional manifold to the lower-dimensional one and preserving local neighbourhoods at every point of the underlying manifold. In recent years, the so-called autoencoder (AE) technique, a capable ML-based algorithm for dimensionality reduction and feature learning (Hinton and Salakhutdinov, 2006; Goodfellow *et al.*, 2016), is widely and successfully applied to fault diagnosis and anomaly detection (Jiang *et al.*, 2017; Ahmed *et al.*, 2022; Hu *et al.*, 2022; Liu *et al.*, 2021; Ren *et al.*, 2020). An AE consists of an encoder and a decoder, where the encoder compresses the data in the higher-dimensional space into a lower-dimensional feature manifold represented by the so-called latent variable, and the decoder is driven by the latent variable and delivers the process variables reflecting, in case of fault diagnosis, nominal process operations. The encoder and decoder are constructed using neural networks (NNs) that are learnt in such a way that the latent variable (the lower-dimensional feature) contains exclusive informations of the nominal process dynamics, from which the process variables in the nominal state are then fully reconstructed. To put it in a nutshell, dimensionality reduction is a capable strategy to remove redundant and irrelevant informations in the data and thus recover exclusive information about the nominal process operations by means of projecting the data in the higher-dimensional space to the lower-dimensional feature manifold.

A comparison of the observer-based and dimensionality reduction-based ML diagnose methods reveals the following insightful differences of these fault detection strategies, in spite of the evidently different assumptions on the types of available process knowledge and information,

- the input-output/state space models describing the nominal system dynamics build the system core of observer-based fault detection, while the ML-based methods handle the nominal system dynamics as a sub-manifold (feature manifold) embedded in the (higher-dimensional) data space composed of all the process data with uncertainties,
- accordingly, the observer-based methods handle system uncertainties by means of residual generation, and the ML-based methods make use of projection techniques,
- and consequently, in the framework of the observer-based fault detection the detection decision is made on the basis of a norm-based residual evaluation, while for the ML-based methods, the decision is based on the distance metric between the current data vector and the lower-dimensional feature manifold. It is noteworthy that in non-Euclidean space the concept of a geodesic distance is often applied in order to capture the nonlinear structure of the data manifold.

In a short form, these major differences are summarised as

$$\langle \text{I/O-model, residual, norm-based evaluation} \rangle \text{ vs.} \\ \langle \text{feature manifold, projection, geodesic distance} \rangle ,$$

whose centerpiece is handling of nominal dynamics and uncertainties.

Handling of model uncertainties using the projection technique in a Hilbert subspace is nothing new in control theory. In the 90s, gap metric was widely applied in robust control theory to measure influences of model uncertainties on a feedback control system (Georgiou and Smith, 1990; Vinnicombe, 2000). Roughly speaking, a gap is a similarity metric between subspaces in Hilbert space based on an orthogonal projection (Georgiou, 1988; Vinnicombe, 2000; Feintuch, 1998). Applied to robust control theory, a gap metric gives, for instance, the "distance" between the system dynamics with and without uncertainties. The use of gap metrics to fault detection was proposed by (Ding, 2015), and comprehensively investigated in (Li and Ding, 2020; Wang *et al.*, 2022). Motivated by the promising results in these works and inspired by the aforementioned ML-based fault detection methods, an initial project has been launched to investigate application of orthogonal projection technique to fault detection in LTI systems (Ding *et al.*, 2022). The primary objective of the project is to establish a projection-based fault detection technique as a potential alternative framework to the observer-based one and to compare the capacity of the two detection schemes. Below are two distinct conclusions,

- in the projection-based fault detection framework, residual generation and evaluation can be well realised in an optimal and integrated manner, and
- a projection-based fault detection system can be, under certain conditions, equivalently realised by a class of optimal observer-based fault detection systems.

The theoretical basis for these conclusions is the orthogonal projection in Hilbert space which allows an orthogonal decomposition of a process data vector into an optimal estimate (projection) and the residual. As a result, the norms of the process data, the residual vector and the projection satisfy, following the Pythagorean Theorem, the Pythagorean equation, which leads to an optimal fault detection.

Motivated and driven by the aforementioned preliminary results, the main project has started with the objective of establishing a projection-based fault diagnosis framework, in which nonlinear dynamic systems with uncertainties are considered, and an optimal system performance-oriented fault detection as well as fault estimation are defined and approached. This is also the major objective of this draft reporting the main results of our work. We would like to mention that the overall goal of our efforts is to build a uniform framework, in which both control theory based and ML-based methods can be developed for fault diagnosis in dynamic control systems. To be specific, the design of ML-based fault diagnosis systems could be well guided by known control-theoretic knowledge and, on the other hand, the design and realisation of model-based fault diagnosis systems are supported by data-driven and ML-algorithms. Our recent work on control theoretically explainable application of autoencoder methods to fault detection (Li *et al.*, 2022) is an example of the former case, while the latter is inspired by current research on physics-informed machine learning (PINN) (Karniadakis *et al.*, 2021).

To approach the above described objective, we focus on the following four major tasks.

- Definition of nominal system dynamics as a manifold in the process data space and realisation of normalised image and kernel representations. Let the process input and output data build a data space. It is known that, for linear systems, the so-called (stable) image and kernel representations (SIR and SKR) are system model forms that

are equivalent to the input-output (transfer function) and the associated state space models (Vinnicombe, 2000). In particular, the normalised SIR and SKR, as inner and co-inner systems (Hoffmann, 1996), play an importance role in the (orthogonal) projection related research (Georgiou, 1988; Vinnicombe, 2000; Feintuch, 1998). By means of SIR and SKR, two equivalent subspaces, the image and kernel subspaces, are defined in Hilbert space. The analogue concepts are also well defined for nonlinear systems (van der Schaft, 2000). Nevertheless, the lossless properties of inner and co-inner (refer to Definition 2) are of special importance in our subsequent study and motivate us to follow the works by van der Schaft and his co-worker on nonlinear systems (Scherpen and van der Schaft, 1994; Ball and van der Schaft, 1996; Petersen and der Schaft, 2005). The core of these works is various configurations of the so-called Hamiltonian extension (Crouch and van der Schaft, 1987) as Hamiltonian systems, which serve as the major system theoretical tool in our work as well.

- Design and analysis of projection systems. For LTI systems, the orthogonal projection onto the image space is a series system composed of the normalised SIR and its conjugate (Georgiou, 1988). To our best knowledge, no study has been reported about analogue results for nonlinear systems, possibly for the reason that for nonlinear systems such a projection is not a geodesic one and thus seems useless. Despite that, we propose to configure the projection as a Hamiltonian system using the normalised SIR. The centerpiece in this work is undoubtedly the Hamiltonian function of the system, which describes the system dynamics in the sense of energy transfer in the system (Scherpen and van der Schaft, 1994; Ball and van der Schaft, 1996; Petersen and der Schaft, 2005), and is thus interpreted as a system performance function. Associated with it, a key concept, the so-called Legendre transform, is introduced, which gives a dual relation of the input and output vectors of the Hamiltonian system as well as a dual form of the Hamiltonian system (Petersen and der Schaft, 2005; Amari, 2016). For our purpose of fault detection, the dual pair of the Hamiltonian functions is analysed corresponding to the nominal system operation and operations when uncertainties or even faults exist. Although this task is primarily dedicated to construct projection systems, it serves as the system-theoretic basis for the next task as well.
- Bregman divergence-based performance-oriented fault detection. While the first two tasks are, more or less, extended applications of the existing methods, this task is crucially different from the projection-based scheme for LTI systems, where the residual is built by means of the difference of the data vector and its projection and further norm-based evaluated. This task is devoted to three issues: (i) handling of process data in non-Euclidean space aiming at classification, (ii) performance-oriented fault detection, and (iii) interpretation of the projection-based method. To this end, Bregman divergences (Bregman, 1967) are introduced. A Bregman divergence is defined in terms of a convex function and serves as a measure of difference between two points in a space. We propose to define Bregman divergences in terms of Hamiltonian functions. The idea behind that is to measure the difference between the data vector and its projection with respect to the change in the Hamiltonian function as a performance function under consideration. Observe that Bregman divergences form an important class of divergences and are widely used in information geometry (Amari, 2016). In particular, a Bregman divergence together with a Legendre transform may induce a dually flat Riemannian manifold in the data space that may be regarded as a dualistic

extension of the Euclidean space (Amari, 2016; Nielsen, 2020). In this context, the interpretation of the Hamiltonian system based projection as a geodesic projection will be studied.

- Modelling of data uncertainty, manifold of uncertain data, and fault detection and estimation. In the projection-based fault diagnosis framework for LTI systems, thanks to the Pythagorean Theorem and the Pythagorean equation, projections onto the image subspace and its orthogonal complement are dual problems and can be addressed, in a certain sense, in a uniform manner. For process data in a non-Euclidean space, they cannot be decomposed into two components representing nominal and uncertain/faulty data, respectively. In other words, nominal data are corrupted with uncertain data and they are inseparable. For our purposes, the concepts of (data) uncertainty model and manifold of uncertain data are introduced on the basis of SKR. While the data in the image manifold are created under nominal system dynamics, the data in the manifold of uncertain data are assumed to contain uncertainties exclusively. In this sense, the SKR-based uncertainty model is a dual form of the SIR-based model for nominal dynamics. Here, we place a greater emphasis on the possible interpretation of uncertainties as faults. In such a system setting, Hamiltonian systems, the associated Hamiltonian functions and the corresponding Bregman divergences, dual to the ones defined in previous tasks, are defined, designed, and then applied for the fault detection purpose. In addition, on the assumption that the uncertainty is caused by faulty operations, the SKR-based projection onto the manifold of uncertain data delivers an estimate for the faulty data. The performance of such an estimation will finally be analysed.

The intended contributions of our work can be summarised in three levels and are described as follows.

- Establishment of a fault diagnosis framework. This framework provides us with an optimal design of fault diagnosis systems for dynamic control systems, as an alternative to the observer-based one. More importantly, its application is not limited to the design of model-based fault diagnosis systems, but also useful to guide the construction of ML-based fault diagnosis systems.
- Novel fault diagnosis schemes and methods. On the basis of normalised SIR and SKR and the associated projection systems, performance-oriented optimal fault detection and faults estimation are achieved. To this end, a design procedure is proposed that combines the control theoretic methods, Hamiltonian systems with the associated Hamiltonian functions as well as inner and co-inner systems, and the methods known in information geometry like Bregman divergences and Legendre transform. The latter gives an interpretation of the projection onto the system image manifold as a geodesic projection in the context of a dually flat Riemannian manifold. In addition, a fault estimation scheme is proposed on the basis of the concepts of the uncertainty model and manifold of uncertain data.
- Applications of the developed novel fault diagnosis schemes and methods lead to numerous new results, including,
 - determination of the Hamiltonian functions with respect to the nominal dynamics and dynamics corrupted with uncertainties/faults, as given in Theorem 4, Corollary 1 as well as Theorem 8 and Corollary 2,

- determination of Bregman divergences as evaluation functions, corresponding to the projections onto the image manifold and the manifold of uncertain data, proved in Theorem 5 and shown in (98), respectively,
- proof of the interpretation that the projection onto the image manifold is a geodesic projection, as given in Theorem 6,
- proof of Theorem 7 that shows the evaluation function over a time interval is a Bregman divergence as well,
- proof of the interpretation of the projection onto the manifold of uncertain data as a geodesic projection, given in Theorem 9, and
- demonstration of the projections onto the manifold of uncertain data as a least square (LS) estimation subject to the uncertainty model in Subsection 4.3.2.

The draft is organised as follows. In Section 2, necessary preliminaries are introduced. At first, the orthogonal projection-based fault detection scheme for LTI systems, serving as background and inspiration, is briefly reviewed. Further control-theoretic preliminaries include image and kernel representations of nonlinear dynamic systems, Hamiltonian systems, inner and co-inner systems. It is followed by an introduction to definitions and computation of Bregman divergences and Legendre transform. They are used not only as divergences for performance-oriented fault detection, but also for inducing a dual Riemannian structure in the data space, which admits a conjugate pair of affine connections. In this regard, the concepts of divergences from a (data) vector to a manifold and geodesic projections are described. At the end of this section, problems to be addressed in this draft are specified. Section 3 is devoted to the projection and Bregman divergence based fault detection. This work consists of three parts. The first part deals with construction of a projection system by means of the normalised SIR and its associated Hamiltonian systems, and the analysis of the corresponding Hamiltonian functions under different operation conditions. It is followed by the second part focusing on (i) computation of the Bregman divergence from the data vector to its projection, which is derived from the (dual) Hamiltonian function, (ii) its use for fault detection, and (iii) its interpretation as a geodesic projection. The last part in this section discusses about implementations issues, including definition of a reliable evaluation function over an evaluation time interval and determination of a threshold. In Section 4, two different but strongly related topics are addressed. The first one is an SKR-based projection, as a dual fault detection scheme to the SIR-based projection. This work is analogue to the one presented in Section 3. Fault estimation is the second topic. The focus of this study is on the application of an SKR-based projection as a fault estimator and analysis of its estimation performance. For both parts, the so-called uncertainty model and the manifold of uncertain data serve as a common basis and are introduced at the beginning of this section.

Throughout this paper, standard notations known in advanced control theory and linear algebra are adopted. In addition, \mathcal{L}_2 is time domain space of all square summable Lebesgue signals (signals with bounded energy). For a transfer matrix $G(s)$, its conjugate is denoted by $G^\sim(s)$ ($= G^T(-s)$). In the context of Legendre transform, the dual of vector α and function φ is denoted by α^\times and φ^\times , respectively. Spaces and manifolds are denoted by calligraphic letters such as \mathcal{I}, \mathcal{K} for image and kernel subspaces (manifolds).

2 Preliminaries

2.1 System factorisations and projection-based fault detection of LTI systems

Consider an LTI system modelled by a transfer function matrix $G(s)$, whose minimal state space representation is given by

$$G : \begin{cases} \dot{x}(t) = Ax(t) + Bu(t) \\ y(t) = Cx(t) + Du(t), \end{cases}$$

where $x \in \mathbb{R}^n, u \in \mathbb{R}^p, y \in \mathbb{R}^m$ are the state, input and output vectors, respectively, A, B, C, D are system matrices of appropriate dimensions. A right coprime factorisation (RCF) of G is given by $G(s) = N(s)M^{-1}(s)$ with the right coprime pair (M, N) whose state space representations are given by

$$M(s) = (A + BF, BV, F, V), N(s) = (A + BF, BV, C + DF, DV). \quad (1)$$

where F is selected such that $A + BF$ is Hurwitz, V as a pre-filter is an invertible constant matrix. The RCF of G can be interpreted as a state feedback control system with $u = Fx + Vv$, where v serves as a reference signal. An alternative model form of $y = Gu$ is the so-called stable image representation (SIR) (Ding, 2020; van der Schaft, 2000) expressed in terms of (M, N) by

$$I_G(s) : \begin{bmatrix} u(s) \\ y(s) \end{bmatrix} = \begin{bmatrix} M(s) \\ N(s) \end{bmatrix} v(s). \quad (2)$$

In this context, vector v is understood as a latent variable.

Remark 1 *Hereafter, we may drop out the domain variable s or t when there is no risk of confusion.*

The dual concepts to RCF and SIR are the so-called left coprime factorisation (LCF) and stable kernel representation (SKR) of G (Vinnicombe, 2000). Denoted by

$$K_G(s) = \begin{bmatrix} -\hat{N}(s) & \hat{M}(s) \end{bmatrix}$$

with (\hat{M}, \hat{N}) as a left coprime pair, the state space realisation of K_G is

$$K_G : \begin{cases} \dot{\hat{x}} = (A - LC)\hat{x} + \begin{bmatrix} B - LD & -L \end{bmatrix} \begin{bmatrix} u \\ y \end{bmatrix} \\ r_y = -WC\hat{x} + \begin{bmatrix} -WD & W \end{bmatrix} \begin{bmatrix} u \\ y \end{bmatrix}, \end{cases}$$

which is an observer-based residual generator with r_y as the residual vector satisfying

$$r_y = Wr_0, r_0 = y - C\hat{x} - Du.$$

As an observer-based residual generator, the observer gain L is selected such that $A - LC$ is Hurwitz, and W is an invertible post-filter. It is obvious that for $\hat{x}(0) = x(0)$, K_G satisfies

$$r_y = K_G \begin{bmatrix} u \\ y \end{bmatrix} = K_G I_G v = 0 \implies \begin{bmatrix} -\hat{N} & \hat{M} \end{bmatrix} \begin{bmatrix} M \\ N \end{bmatrix} = 0. \quad (3)$$

During normal process operations, the process data (u, y) build a subspace in Hilbert space \mathcal{L}_2 , called image subspace of G , which is explicitly defined by the SIR of G and the latent variable v as follows

$$\mathcal{I}_G = \left\{ \begin{bmatrix} u \\ y \end{bmatrix} : \begin{bmatrix} u \\ y \end{bmatrix} = \begin{bmatrix} M \\ N \end{bmatrix} v, v \in \mathcal{L}_2 \right\}. \quad (4)$$

By means of K_G , the kernel subspace of G is defined as

$$\mathcal{K}_G = \left\{ \begin{bmatrix} u \\ y \end{bmatrix} : r_y = \begin{bmatrix} -\hat{N} & \hat{M} \end{bmatrix} \begin{bmatrix} u \\ y \end{bmatrix} = 0, \begin{bmatrix} u \\ y \end{bmatrix} \in \mathcal{L}_2 \right\}, \quad (5)$$

which is, due to relation (3), identical with \mathcal{I}_G , i.e. $\mathcal{K}_G = \mathcal{I}_G$ (Vinnicombe, 2000). The complementary subspace of \mathcal{I}_G is denoted by \mathcal{I}_G^\perp .

Let

$$I_{G,0}(s) = \begin{bmatrix} M_0(s) \\ N_0(s) \end{bmatrix}, K_{G,0}(s) = \begin{bmatrix} -\hat{N}_0(s) & \hat{M}_0(s) \end{bmatrix}$$

denote the normalised SIR and SKR of G , defined by

$$I_{G,0}^\sim I_{G,0} = N_0^\sim N_0 + M_0^\sim M_0 = I, K_{G,0} K_{G,0}^\sim = \hat{N}_0 \hat{N}_0^\sim + \hat{M}_0 \hat{M}_0^\sim = I. \quad (6)$$

On account of (3) and (6), we have

$$\begin{bmatrix} I_{G,0}^\sim \\ K_{G,0} \end{bmatrix} \begin{bmatrix} I_{G,0} & K_{G,0}^\sim \end{bmatrix} = \begin{bmatrix} M_0^\sim & N_0^\sim \\ -\hat{N}_0 & \hat{M}_0 \end{bmatrix} \begin{bmatrix} M_0 & -\hat{N}_0^\sim \\ N_0 & \hat{M}_0^\sim \end{bmatrix} = \begin{bmatrix} I & 0 \\ 0 & I \end{bmatrix}. \quad (7)$$

The reader is referred to (Hoffmann, 1996) for more details about the normalised SIR and SKR and their computation. It is noteworthy that the normalised SIR and SKR of G are so-called inner and co-inner systems, respectively (Hoffmann, 1996).

Now, we are in a position to introduce the basic idea and algorithms of projection-based optimal fault detection system. Let $\mathcal{P}_\mathcal{V}$ be an operator defined on a subspace \mathcal{V} in Hilbert space that is endowed with the inner product,

$$\langle \alpha, \beta \rangle = \int_{-\infty}^{\infty} \alpha^T(t) \beta(t) dt, \alpha, \beta \in \mathcal{V} \subset \mathcal{L}_2.$$

If $\mathcal{P}_\mathcal{V}$ is idempotent and self-adjoint, namely

$$\forall \alpha, \beta \in \mathcal{V}, \mathcal{P}_\mathcal{V}^2 = \mathcal{P}_\mathcal{V}, \langle \mathcal{P}_\mathcal{V} \alpha, \beta \rangle = \langle \alpha, \mathcal{P}_\mathcal{V} \beta \rangle, \quad (8)$$

it is an operator of an orthogonal projection onto \mathcal{V} (Kato, 1995). If the subspace \mathcal{V} is closed, the distance between β and \mathcal{V} , $dist(\beta, \mathcal{V})$, is defined as

$$dist(\beta, \mathcal{V}) = \inf_{\alpha \in \mathcal{V}} \|\beta - \alpha\|_2, \quad (9)$$

which can be computed as

$$dist(\beta, \mathcal{V}) = \|\beta - \mathcal{P}_\mathcal{V} \beta\|_2 = \|\mathcal{P}_{\mathcal{V}^\perp} \beta\|_2.$$

It is well-known that the image subspace \mathcal{I}_G is closed in \mathcal{L}_2 and $\mathcal{P}_{\mathcal{I}_G} : \mathcal{L}_2 \rightarrow \mathcal{L}_2$,

$$\mathcal{P}_{\mathcal{I}_G} \left(\begin{bmatrix} u \\ y \end{bmatrix} \right) := I_{G,0} \tilde{I}_{G,0} \begin{bmatrix} u \\ y \end{bmatrix}$$

defines an orthogonal projection onto \mathcal{I}_G (Vinnicombe, 2000) with $\mathcal{P}_{\mathcal{I}_G}$ denoting the projection operator. Note that operator $\mathcal{I} - \mathcal{P}_{\mathcal{I}_G} : \mathcal{L}_2 \rightarrow \mathcal{L}_2$,

$$(\mathcal{I} - \mathcal{P}_{\mathcal{I}_G}) \begin{bmatrix} u \\ y \end{bmatrix} = (I - I_{G,0} \tilde{I}_{G,0}) \begin{bmatrix} u \\ y \end{bmatrix}, \quad (10)$$

defines an orthogonal projection onto the orthogonal complement of \mathcal{I}_G . Consequently, any process data can be written as

$$\begin{bmatrix} u \\ y \end{bmatrix} = \mathcal{P}_{\mathcal{I}_G} \begin{bmatrix} u \\ y \end{bmatrix} + \mathcal{P}_{\mathcal{I}_G^\perp} \begin{bmatrix} u \\ y \end{bmatrix}, \mathcal{P}_{\mathcal{I}_G^\perp} = \mathcal{I} - \mathcal{P}_{\mathcal{I}_G}.$$

In the context of one-class classification, faulty operations are detected if

$$\begin{bmatrix} u \\ y \end{bmatrix} \notin \mathcal{I}_G \implies \mathcal{P}_{\mathcal{I}_G^\perp} \begin{bmatrix} u \\ y \end{bmatrix} \neq 0,$$

and $\mathcal{P}_{\mathcal{I}_G^\perp} \begin{bmatrix} u \\ y \end{bmatrix}$ is sufficiently large (with respect to a defined threshold). From the implementation point of view, it is of interest to notice that, due to (7), it holds

$$\begin{aligned} \begin{bmatrix} I_{G,0} & K_{\tilde{G},0} \end{bmatrix} \begin{bmatrix} \tilde{I}_{G,0} \\ K_{G,0} \end{bmatrix} = I &\iff I - I_{G,0} \tilde{I}_{G,0} = K_{\tilde{G},0} K_{G,0} \implies \\ \left\| (\mathcal{I} - \mathcal{P}_{\mathcal{I}_G}) \begin{bmatrix} u \\ y \end{bmatrix} \right\|_2 &= \left\| K_{\tilde{G},0} K_{G,0} \begin{bmatrix} u \\ y \end{bmatrix} \right\|_2 = \left\| K_{G,0} \begin{bmatrix} u \\ y \end{bmatrix} \right\|_2 = \|r_y\|_2. \end{aligned} \quad (11)$$

Consequently, when the \mathcal{L}_2 -norm is used for residual evaluation, the projection $\mathcal{P}_{\mathcal{I}_G}$ and the corresponding residual generation $(\mathcal{I} - \mathcal{P}_{\mathcal{I}_G}) \begin{bmatrix} u \\ y \end{bmatrix}$ can be equivalently realised in the observer-based fault detection framework (Ding, 2008).

In a nutshell, an orthogonal projection onto a subspace in Hilbert space enables us to compute the distance between a collected data and the nominal system operation presented by the image/kernel subspace of the system under consideration. Thanks to the orthogonality, it holds

$$\begin{aligned} \begin{bmatrix} u \\ y \end{bmatrix} &= \mathcal{P}_{\mathcal{I}_G} \left(\begin{bmatrix} u \\ y \end{bmatrix} \right) + \mathcal{P}_{\mathcal{I}_G^\perp} \begin{bmatrix} u \\ y \end{bmatrix} \implies \\ \left\| \begin{bmatrix} u \\ y \end{bmatrix} \right\|_2^2 &= \left\| \mathcal{P}_{\mathcal{I}_G} \left(\begin{bmatrix} u \\ y \end{bmatrix} \right) \right\|_2^2 + \left\| \mathcal{P}_{\mathcal{I}_G^\perp} \left(\begin{bmatrix} u \\ y \end{bmatrix} \right) \right\|_2^2 \implies \\ \|r_y\|_2^2 &= \left\| K_{G,0} \begin{bmatrix} u \\ y \end{bmatrix} \right\|_2^2 = \left\| \begin{bmatrix} u \\ y \end{bmatrix} \right\|_2^2 - \left\| \mathcal{P}_{\mathcal{I}_G} \left(\begin{bmatrix} u \\ y \end{bmatrix} \right) \right\|_2^2, \end{aligned} \quad (12)$$

which results in an optimal fault detection in LTI systems. We would like to emphasise that this scheme is a one-class fault detection, which is achieved solely based on the nominal system dynamics. An extension to two-class fault detection as well as to fault isolation (multi-class classification) is straightforward (Ding *et al.*, 2022).

2.2 Kernel and image representations of nonlinear systems, and manifolds

A nonlinear dynamic system Σ can be generally modelled as

$$\Sigma : \begin{cases} \dot{x}(t) = f(x(t), u(t)) \\ y(t) = h(x(t), u(t)), \end{cases}$$

where $x \in \mathbb{R}^n$ denotes the state vector, $u \in \mathbb{R}^p$ and $y \in \mathbb{R}^m$ represent system input and output vectors, respectively. $f(x, u)$ and $h(x, u)$ are continuously differentiable nonlinear functions with appropriate dimensions. In our work, for the sake of simplicity, the affine form of Σ ,

$$\Sigma : \begin{cases} \dot{x} = a(x) + B(x)u, x(0) = x_0 \\ y = c(x) + D(x)u, \end{cases} \quad (13)$$

is under consideration. Here, x_0 represents the initial value of $x(t)$, and $a(x)$, $B(x)$, $c(x)$ and $D(x)$ are continuously differentiable and of appropriate dimensions. The affine system (13) is a class of nonlinear systems which are widely adopted in nonlinear system research and can be considered as a natural extension of linear systems.

Roughly speaking, given system Σ , a stable system $\Sigma_{\mathcal{I}}$ is a stable image representation (SIR) of Σ if for all \mathcal{L}_2 -bounded input u and its \mathcal{L}_2 -bounded response $y = \Sigma(u)$, there exists an \mathcal{L}_2 -bounded $v \in \mathbb{R}^p$ such that (van der Schaft, 2000)

$$\begin{bmatrix} u \\ y \end{bmatrix} = \Sigma_{\mathcal{I}}(v).$$

The state space representation of the SIR $\Sigma_{\mathcal{I}}(v)$ is an essential model form used in our subsequent work and is given by

$$\Sigma_{\mathcal{I}} : \begin{cases} \dot{x} = a_I(x) + B_I(x)v \\ \begin{bmatrix} u \\ y \end{bmatrix} = c_I(x) + D_I(x)v, \end{cases} \quad (14)$$

$$a_I(x) = a(x) + B(x)g(x), B_I(x) = B(x)V(x),$$

$$c_I(x) = \begin{bmatrix} g(x) \\ c(x) + D(x)g(x) \end{bmatrix}, D_I(x) = \begin{bmatrix} V(x) \\ D(x)V(x) \end{bmatrix},$$

where $g(x)$ is designed such that $a_I(x)$ is stable, and $V(x) \in \mathbb{R}^{p \times p}$ is invertible. In the context of feedback control systems,

$$u = g(x) + V(x)v$$

is understood as a controller with a state feedback $g(x)$, feed-forward controller $V(x)$ and v as the reference signal. Note that

$$D_I^T(x)D_I(x) = V^T(x) (I + D^T(x)D(x)) V(x)$$

is invertible.

The so-called stable kernel representation (SKR) of Σ is another system model form and useful in our subsequent study. The SKR of Σ , denoted by $\Sigma_{\mathcal{K}}$, is a stable system that satisfies, roughly speaking,

$$r_y = \Sigma_{\mathcal{K}} \begin{pmatrix} u \\ y \end{pmatrix} = 0, r_y \in \mathbb{R}^m, \quad (15)$$

when there exists no uncertainty in the system. The state space representation of SKR $\Sigma_{\mathcal{K}}$ is described by

$$\Sigma_{\mathcal{K}} : \begin{cases} \dot{\hat{x}} = a(\hat{x}) + B(\hat{x})u + L(\hat{x})(y - \hat{y}), \hat{x}(0) = \hat{x}_0 \\ \quad = a_K(\hat{x}) + B_K(\hat{x}) \begin{bmatrix} u \\ y \end{bmatrix} \\ r_y = W(\hat{x})r_0 = c_K(\hat{x}) + D_K(\hat{x}) \begin{bmatrix} u \\ y \end{bmatrix} \\ r_0 = y - \hat{y}, \hat{y} = c(\hat{x}) + D(\hat{x})u, \end{cases} \quad (16)$$

$$a_K(\hat{x}) = a(\hat{x}) - L(\hat{x})c(\hat{x}), B_K(\hat{x}) = [B(\hat{x}) - L(\hat{x})D(\hat{x}) \quad L(\hat{x})],$$

$$c_K(\hat{x}) = -W(\hat{x})c(\hat{x}), D_K(\hat{x}) = [-W(\hat{x})D(\hat{x}) \quad W(\hat{x})],$$

where $L(\hat{x})$ is designed such that $a_K(\hat{x})$ is stable and $W(\hat{x}) \in \mathbb{R}^{m \times m}$ is invertible. In the detection context, r_0 builds a residual vector, W is a post-filter, and it holds

$$D_K^T(\hat{x})D_K(\hat{x}) = W(\hat{x})(I + D(\hat{x})D^T(\hat{x}))W^T(\hat{x})$$

being invertible. Note that for $\hat{x}(0) = \hat{x}_0 = x(0) = x_0, r_y = r_0 = 0$. For this case, we denote $\Sigma_{\mathcal{K}}$ by $\Sigma_{\mathcal{K}}^{x_0}$. It is apparent that $\forall v$,

$$\Sigma_{\mathcal{K}}^{x_0} \circ \Sigma_{\mathcal{I}}(v) = \Sigma_{\mathcal{K}}^{x_0} \begin{pmatrix} u \\ y \end{pmatrix} = 0 \implies \Sigma_{\mathcal{K}}^{x_0} \circ \Sigma_{\mathcal{I}} = 0. \quad (17)$$

In terms of the concepts of SIR and SKR, we are in a position to introduce the definitions of image and kernel manifolds. They are lower-dimensional manifolds embedded in the data space of (u, y) . This manner of modelling dynamic systems enables us to address fault detection/classification issues directly in the data space, rather than on the basis of the system input-output relations.

Definition 1 *Given system (13), its SIR (14) and SKR (16),*

$$\mathcal{I}_{\Sigma} = \left\{ \begin{bmatrix} u \\ y \end{bmatrix} : \begin{bmatrix} u \\ y \end{bmatrix} = \Sigma_{\mathcal{I}}(v), v \in \mathcal{L}_2 \right\}, \quad (18)$$

$$\mathcal{K}_{\Sigma} = \left\{ \begin{bmatrix} u \\ y \end{bmatrix} \in \mathcal{L}_2 : \Sigma_{\mathcal{K}}^{x_0} \left(\begin{bmatrix} u \\ y \end{bmatrix} \right) = 0 \right\} \quad (19)$$

are called image and kernel sub-manifold of Σ , respectively.

Note that, due to relation (17), it holds $\mathcal{I}_{\Sigma} = \mathcal{K}_{\Sigma}$.

2.3 Hamiltonian, inner systems, and normalised SIR and SKR

Recall that for LTI systems, the normalised SIR and SKR are defined in terms of the transfer functions of the RCF and LCF as well as their conjugates. For nonlinear systems, the well-established Hamiltonian system technique can be applied for this purpose. In a broad sense, given a nonlinear system as an operator, the associated Hamiltonian system can be interpreted as a certain configuration of the operator and its adjoint. In this regard, we first introduce some essential concepts and definitions known in the literature.

2.3.1 Hamiltonian systems

Consider the affine system (13) and assume that it is stable. The Hamiltonian extension of Σ , introduced in (Crouch and van der Schaft, 1987), is a dynamic system described by

$$\begin{cases} \dot{x} = a(x) + B(x)u \\ \dot{\lambda} = - \left(\frac{\partial a(x)}{\partial x} + \frac{\partial B(x)}{\partial x} u \right)^T \lambda - \left(\frac{\partial c(x)}{\partial x} + \frac{\partial D(x)}{\partial x} u \right)^T u_a \\ y = c(x) + D(x)u \\ y_a = B^T(x)\lambda + D^T(x)u_a, y_a \in \mathbb{R}^p, u_a \in \mathbb{R}^m, \end{cases} \quad (20)$$

with state variables (x, λ) , input variables (u, u_a) and output variables (y, y_a) . $\lambda \in \mathbb{R}^n$ is also called co-state variable. Connecting y and u_a , $u_a = y = c(x) + D(x)u$, and defining a Hamiltonian function

$$H(x, \lambda, u) = \frac{1}{2} (c(x) + D(x)u)^T (c(x) + D(x)u) + \lambda^T (a(x) + B(x)u)$$

lead to the Hamiltonian system $y_a = (D\Sigma)^T \circ \Sigma(u)$, whose state space representation can be written in a compact form

$$(D\Sigma)^T \circ \Sigma : \begin{cases} \dot{x} = \frac{\partial H}{\partial \lambda}(x, \lambda, u) \\ \dot{\lambda} = -\frac{\partial H}{\partial x}(x, \lambda, u) \\ y_a = \frac{\partial H}{\partial u}(x, \lambda, u) \end{cases} \quad (21)$$

with input vector u and output vector y_a . Here, $D\Sigma$ denotes the Frechet derivative of Σ (Crouch and van der Schaft, 1987). Differently, connecting u and y_a of the Hamiltonian extension (20), namely $u = y_a = B^T(x)\lambda + D^T(x)u_a$, results in

$$\Sigma \circ (D\Sigma)^T : \begin{cases} \dot{x} = a(x) + B(x) (B^T(x)\lambda + D^T(x)u_a) \\ \dot{\lambda} = - \left(\frac{\partial a(x)}{\partial x} + \frac{\partial \bar{B}(x, \lambda, u_a)}{\partial x} \right)^T \lambda - \left(\frac{\partial c(x)}{\partial x} + \frac{\partial \bar{D}(x, \lambda, u_a)}{\partial x} \right)^T u_a \\ y = c(x) + D(x)B^T(x)\lambda + D(x)D^T(x)u_a, \\ \bar{B}(x, \lambda, u_a) = B(x) (B^T(x)\lambda + D^T(x)u_a), \\ \bar{D}(x, \lambda, u_a) = D(x)B^T(x)\lambda + D(x)D^T(x)u_a. \end{cases} \quad (22)$$

Let

$$H(x, \lambda, u_a) = \frac{1}{2} u_a^T D(x)D^T(x)u_a + c^T(x)u_a + \lambda^T \left(a(x) + \frac{1}{2} B(x)B^T(x)\lambda + B(x)D^T(x)u_a \right) \quad (23)$$

be a Hamiltonian function. Accordingly, $\Sigma \circ (D\Sigma)^T$ can be compactly written as

$$\Sigma \circ (D\Sigma)^T : \begin{cases} \dot{x} = \frac{\partial H}{\partial \lambda}(x, \lambda, u_a) \\ \dot{\lambda} = -\frac{\partial H}{\partial x}(x, \lambda, u_a) \\ y = \frac{\partial H}{\partial u_a}(x, \lambda, u_a). \end{cases} \quad (24)$$

2.3.2 Inner and co-inner, normalised SIR and SKR

As mentioned in Subsection 2.1, for LTI systems, the normalised SIR and SKR are inner and co-inner, respectively. This motivates us to review the concepts and existence conditions of nonlinear inner and co-inner systems, before addressing the normalised SIR and SKR issues. The presented results can be found e.g. in (Scherpen and van der Schaft, 1994; Ball and van der Schaft, 1996; van der Schaft, 2000).

Definition 2 Consider the stable nonlinear affine system (13). Σ is inner if the Hamiltonian system (21) satisfies

$$y_a = u, \quad (25)$$

and lossless, and it is co-inner, when it holds, for the Hamiltonian system (24),

$$y = u_a \quad (26)$$

and lossless. Here, Σ is called lossless, if there exists a storage function $V(x) \geq 0, V(0) = 0$ so that

$$V(x(t_2)) - V(x(t_1)) = \frac{1}{2} \int_{t_1}^{t_2} (u^T u - y^T y) d\tau. \quad (27)$$

Lemma 1 The nonlinear affine system (13) is inner, if there exists $V(x) \geq 0$ such that the following equations are feasible

$$V_x^T(x) a(x) + \frac{1}{2} c^T(x) c(x) = 0, \quad (28)$$

$$V_x^T(x) B(x) + c^T(x) D(x) = 0, \quad (29)$$

$$D^T(x) D(x) = I, \quad (30)$$

where $V_x(x) = \frac{\partial V(x)}{\partial x}$. And, it is co-inner, if there exists $V(x) \geq 0$ such that the following equations are feasible

$$V_x^T(x) a(x) + \frac{1}{2} V_x^T(x) B(x) B^T(x) V_x(x) = 0, \quad (31)$$

$$c^T(x) + V_x^T(x) B(x) D^T(x) = 0, \quad (32)$$

$$D(x) D^T(x) = I. \quad (33)$$

Definition 3 The SIR $\Sigma_{\mathcal{I}}$ and SKR $\Sigma_{\mathcal{K}}$ given in (14) and (16), respectively, are normalised, when $(g(x), V(x))$ and $(L(x), W(x))$ are set such that $\Sigma_{\mathcal{I}}$ is inner and $\Sigma_{\mathcal{K}}$ is co-inner.

Theorem 1 The SIR (14) is normalised, if there exists $P(x) \geq 0$ such that the following equation is feasible

$$P_x^T(x) a(x) + \frac{1}{2} c^T(x) c(x) - \frac{1}{2} g^T(x) (I + D^T(x) D(x)) g(x) = 0, \quad (34)$$

and $(g(x), V(x))$ are set to be

$$g(x) = - (I + D^T(x)D(x))^{-1} (B^T(x)P_x(x) + D^T(x)c(x)), \quad (35)$$

$$V(x) = V^T(x) = (I + D^T(x)D(x))^{-1/2}. \quad (36)$$

And the SKR (16) is normalised, if there exists $V(\hat{x}) \geq 0$ solving

$$\begin{aligned} & V_{\hat{x}}^T(\hat{x}) a(\hat{x}) + \frac{1}{2} V_{\hat{x}}^T(\hat{x}) B(\hat{x}) B^T(\hat{x}) V_{\hat{x}}(\hat{x}) \\ & - \frac{1}{2} (c^T(\hat{x}) + V_{\hat{x}}^T(\hat{x}) B(\hat{x}) D^T(\hat{x})) (I + D(\hat{x}) D^T(\hat{x}))^{-1} (c^T(\hat{x}) + V_{\hat{x}}^T(\hat{x}) B(\hat{x}) D^T(\hat{x}))^T = 0, \end{aligned} \quad (37)$$

and $(L(x), W(x))$ are set to be

$$V_{\hat{x}}^T(\hat{x}) L(\hat{x}) = (c^T(\hat{x}) + V_{\hat{x}}^T(\hat{x}) B(\hat{x}) D^T(\hat{x})) (I + D(\hat{x}) D^T(\hat{x}))^{-1}, \quad (38)$$

$$W(\hat{x}) = (I + D(\hat{x}) D^T(\hat{x}))^{-1/2}. \quad (39)$$

The proof of this theorem follows immediately from Lemma 1 and thus is omitted.

Remark 2 *The normalised SIR can be interpreted as an optimal controller under a quadric cost function associated to the Hamiltonian functions (van der Schaft, 2000). A normalised SKR based estimator results in a LS estimation of uncertainties corrupted in data (u, y) , as will be demonstrated in Subsection 4.3.*

2.4 Bregman divergence, Legendre transform, and geodesic projection

For our purpose, we restrict our attention to the following definition of a Bregman divergence. Let $\varphi : \mathbb{R}^n \rightarrow \mathbb{R}$ be a continuously-differentiable, strictly convex function. Bregman divergence from $\alpha \in \mathbb{R}^n$ to $\beta \in \mathbb{R}^n$, denoted by $D_\varphi[\alpha : \beta]$, is defined by

$$D_\varphi[\alpha : \beta] = \varphi(\alpha) - \varphi(\beta) - \left(\frac{\partial \varphi(\beta)}{\partial \beta} \right)^T (\alpha - \beta).$$

The function φ is also called generating function. Bregman divergences were introduced by Bregman as a measure of difference between two points in a space (Bregman, 1967). A Bregman divergence is of all properties of a divergence. In our subsequent work, the dual divergence to $D_\varphi[\alpha : \beta]$ plays an important role. To define it, we first consider a Legendre transform. Let

$$\alpha^\times = \frac{\partial}{\partial \alpha} \varphi(\alpha) \in \mathbb{R}^n.$$

The function

$$\varphi^\times(\alpha^\times) := \alpha^T \alpha^\times - \varphi(\alpha)$$

is called the Legendre dual of φ . It is known (Amari, 2016) that

$$\alpha^\times = \frac{\partial}{\partial \alpha} \varphi(\alpha), \quad \alpha = \frac{\partial}{\partial \alpha^\times} \varphi^\times(\alpha^\times),$$

form a dualistic structure, and $\varphi^\times(\alpha^\times)$ is convex with respect to α^\times .

By means of the Legendre dual of φ , the dual divergence to $D_\varphi[\alpha : \beta]$ is defined by

$$D_{\varphi^\times}[\alpha^\times : \beta^\times] = \varphi(\alpha^\times) - \varphi(\beta^\times) - \left(\frac{\partial \varphi^\times(\beta^\times)}{\partial \beta^\times} \right)^T (\alpha^\times - \beta^\times).$$

By some straightforward computations (Amari, 2016), we obtain

$$D_\varphi[\alpha : \beta] = \varphi(\alpha) + \varphi^\times(\beta^\times) - \alpha^T \beta^\times, \quad (40)$$

$$D_{\varphi^\times}[\alpha^\times : \beta^\times] = D_\varphi[\beta : \alpha]. \quad (41)$$

The introduction of the dual divergence is not only useful from the computational point of view. It is the theoretical basis for the definition and computation of the so-called geodesic projection onto a manifold. Informally speaking, a geodesic projection can be understood as an extension of the concept of an orthogonal projection onto a vector subspace. Below, we shortly highlight the basic ideas and some results on the Bregman divergence-based geodesic project described in (Amari, 2016; Nielsen, 2020), and restrict the introduction only to the so-called projection theorem that is needed for our fault detection study. The reader is referred to (Amari, 2016; Nielsen, 2020) and references therein for more details.

In his monograph on Information geometry (Amari, 2016), Amari begins the introduction to a dually flat Riemannian manifold with the following statement, “*we can establish a new edifice of differential geometry, by treating a pair of affine connections which are dually coupled with respect to the Riemannian metric. Such a structure ... is the heart of information geometry. ... As an important special case, we study a dually flat Riemannian manifold. It may be regarded as a dualistic extension of the Euclidean space.*” Given two convex functions connected by the Legendre transform $\alpha^\times = \nabla F(\alpha)$, $\alpha = \nabla F^\times(\alpha^\times)$, Bregman and dual Bregman divergences, $D_\varphi[\alpha : \beta] =: F(\alpha)$, $D_{\varphi^\times}[\alpha^\times : \beta^\times] =: F^\times(\alpha^\times)$ on a manifold \mathcal{M} are defined. On this basis, metric tensors

$$G := \nabla^2 F(\alpha), G^\times := \nabla^2 F^\times(\alpha^\times)$$

provide \mathcal{M} with a dual Riemannian structure that admits a conjugate pair of affine connections. In (Amari, 2016), it is proved that these two affine connections are curvature- and torsion-free, and thus the corresponding Riemannian structure is called dually flat. Consequently, any pair of points in \mathcal{M} can be linked by a straight line either in the coordinate system α or in its dual coordinate system α^\times (Amari, 2016; Nielsen, 2020). A main result related to a dually flat structured manifold is the proof of the Generalised Pythagorean Theorem by Nagaoka and Amari (Nagaoka and Amari, 1982). Based on it, the projection theorem given below was proved (Amari, 2016).

Let $\mathcal{M} \subset \mathbb{R}^n$ denote a dually flat manifold.

Definition 4 Given $\alpha \in \mathcal{M}$ and a submanifold $\mathcal{S} \subset \mathcal{M}$, the divergence from α to \mathcal{S} is defined by

$$D_\varphi[\alpha : \mathcal{S}] = \min_{\beta \in \mathcal{S}} D_\varphi[\alpha : \beta].$$

A curve is said to be orthogonal to \mathcal{S} when its tangent vector is orthogonal to any tangent vectors of \mathcal{S} at the intersection.

Definition 5 $\hat{\alpha}_{\mathcal{S}} \in \mathcal{S}$ is called *geodesic projection of α to \mathcal{S}* when the geodesic connecting α and $\hat{\alpha}_{\mathcal{S}}$ is orthogonal to \mathcal{S} . Dually, $\hat{\alpha}_{\mathcal{S}}^{\times} \in \mathcal{S}$ is the *dual geodesic projection of α to \mathcal{S}* , when the dual geodesic connecting α and $\hat{\alpha}_{\mathcal{S}}^{\times}$ is orthogonal to \mathcal{S} .

Theorem 2 (*Projection theorem, (Amari, 2016), Theorem 1.4*) Given $\alpha \in \mathcal{M}$ and a smooth submanifold \mathcal{S} in a dually flat manifold \mathcal{M} , the vector that minimises the divergence $D_{\varphi}[\alpha : \beta]$, $\beta \in \mathcal{S}$, is the dual geodesic projection of α to \mathcal{S} . The vector that minimises the dual divergence $D_{\varphi^{\times}}[\alpha : \beta]$, $\beta \in \mathcal{S}$, is the geodesic projection of α to \mathcal{S} .

2.5 Problem formulation

The main intention of introducing the system coprime factorisations and the SIR/SKR concepts is to model the (nominal) system dynamic as a subspace/sub-manifold in the data space of (u, y) . Although these model forms are equivalent to the input-output models widely applied in control theoretic research, they provide us with the alternative methodology to deal with fault diagnosis problems, namely directly in data space and by means of an orthogonal projection. As delineated by the projection-based fault detection scheme for LTI systems (Ding *et al.*, 2022), an orthogonal projection of (u, y) onto the system image (kernel) subspace helps us to extract information from the data optimally using the distance of the data vector to the system image subspace as the (nominal) system dynamics. In this regard, the normalised SIR and SKR serve for two purposes. Firstly, it is a mathematical tool for the computation of the projection and the distance. Secondly, it connects the projection-based fault detection with the observer-based one, as expressed by (7) and, in particular, (12). The latter implies that the projection-based fault detection can be realised using an observer-based detection system and thus, on the other hand, enables an optimal design of an observer-based detection system.

A direct extension of the projection-based fault detection to nonlinear dynamic systems poses obviously a number of problems. While the SIR and SKR can be, analogue to LTI systems, straightforward introduced, concepts like projection and distance definitions have to be addressed with the aid of different mathematical tools and knowledge. Concerning projection issues, the well-established theoretic framework of Hamiltonian systems (Scherpen and van der Schaft, 1994; Ball and van der Schaft, 1996; van der Schaft, 2000) may serve as the system foundation, and as an analysis and computational tool, where the Hamiltonian systems corresponding to the normalised SIR and SKR and their solutions as inner and co-inner systems play an important role in our subsequent work. The centerpiece in our framework is the associated Hamiltonian functions, by which the Bregman divergences are introduced for our fault detection study.

To be specific, for LTI systems, the system image (kernel) is a subspace in Hilbert space, in which an inner product and the corresponding norm of a vector are well defined. In such a Euclidean space, the shortest distance between two points (vectors) is a straight line, and thus the norm of a residual vector is efficient for measuring the distance from a data vector to the system image subspace that represents the nominal dynamics. This is the theoretic basis for an optimal fault detection. In a non-Euclidean space, as the manifold formed by

process data from a nonlinear system, the metric tensor at each point of the manifold is different from the Euclidean metric tensor like an inner product defined on Hilbert space. Therefore, the norm-based distance defined in Hilbert space may not be compatible with the metric tensor of the non-Euclidean space. In other words, the norm-based metric is not suitable to measure the distance from a data vector to the system image manifold, based on which a fault detection should be made. To solve this problem, we propose to use Bregman divergences to measure deviations in the system dynamics and data from the nominal ones. Initially, this idea has been inspired by wide applications of Bregman divergences in machine learning (Adamcik, 2014; Frigyik *et al.*, 2008) and, in particular, the Kullback-Leibler (KL) divergence as a difference measure of two probability distributions. In course of our extensive investigation, three distinguishing aspects of applying Bregman divergences to fault detection draw our attention : (i) realisation of performance-oriented fault detection, (ii) simplified computation and realisation of Bregman divergences making use of the dual Hamiltonian system pair as a Legendre transform, and (iii) interpretation of the SIR-based projection as a geodesic projection in terms of Bregman divergence from a data vector to the image manifold. To be specific,

- performance-oriented fault detection has been proposed in our earlier works (Li *et al.*, 2019; Li *et al.*, 2020; Ding, 2020), dedicated to reliably detecting performance degradation in automatic control systems. It has been observed that considerable engineering efforts are often needed to set the parameters of the performance evaluation function. Bregman divergences are induced by convex functions and measure the difference of two points (vectors) defined in terms of this convex function. In optimal control, Hamiltonian functions act as (control) performance cost functions. In a broad sense, Hamiltonian functions can be interpreted as the energy balance (parity relation) in dynamic systems. This fact motivates us to define the Hamiltonian function of the system under consideration as a system performance and, based on it, to induce Bregman divergences towards a performance-oriented fault detection.
- It is known that for a given system, there exists a dual Hamiltonian system pair that forms a Legendre transform. As delineated in Subsection 2.4, the Legendre dual of the Hamiltonian functions is useful for the Bregman divergence computations. More importantly, the Bregman divergence endows the data manifold with a dually flat structured Riemannian manifold, which can be regarded as a dualistic extension of the Euclidean space. And thus,
- the projection theorem (Amari, 2016), Theorem 2, can be used to characterise the Hamiltonian function-based projection and to highlight its insight from the viewpoint of information geometry.

As described in Subsection 2.1, a distinguishing feature for projections in Hilbert space is that the vector can be decomposed as the orthogonal projection of the data vector onto the image subspace and its complementary. It leads to the useful relations (7) and (12) that enable to realise a projection-based fault detection system in the well-established observer-based detection framework (refer to (12), the Pythagorean equation). Moreover, they pose a novel scheme to design observer-based fault detection systems that are capable to deal with systems with model uncertainties and multiplicative faults (Ding *et al.*, 2022). Unfortunately, for nonlinear systems such relations are generally not valid. Bearing this fact in mind, we will

study the (nonlinear) SIR- and SKR-based projections separately. The SIR-based projection, similar to the application to LTI systems, concerns with the projection of process data (u, y) to the system image manifold representing the nominal dynamics. By means of a Hamiltonian function induced Bregman divergence, the projection is evaluated, which delivers a distance measure between the data and the image manifold and is used for fault detection. As described in Subsections 2.1 and 2.2, an SKR is an observer-based residual generator that reflects influences of uncertainties in the system, including faults, on the system dynamics. Correspondingly, the SKR-based projection is an estimate for uncertainties. For the fault detection purpose, the evaluation of the SKR-based projection in terms of a Hamiltonian function induced Bregman divergence will be dedicated to a measure of the distance between the data and the uncertainty-free operation.

In course of our study on the SKR-based projection, the imperative of insightfully understanding the SKR-based projection as an estimate for uncertainties has been recognised. Remember that the essential reason why the relation (12) doesn't hold for nonlinear systems is that the data (u, y) are inextricably corrupted with uncertainties. Consequently, the influences of the system input (representing the nominal dynamic) and uncertainties in the system are not separable in the data. As will be shown in Section 4, an SKR-based projection is a Hamiltonian system with the system data (u, y) (equivalent with an observer-based residual generator) as its input and the projection as its output. Our endeavour, to be specific, is to figure out in which context the projection delivers an estimate of the uncertainty corrupted in the data. To this end, an uncertainty model is introduced, which uniformly models deviations in the data from their nominal values and caused by all types of possible uncertainties, including faults. In this regard, it will be delineated that the SKR-based projection is an LS estimate of the uncertainty corrupted in the data. This result not only highlights the insightful interpretation of the SKR-based projection, but also underlines its potential use, for instance, for fault estimation.

To put it in a nutshell, the main problems to be addressed in this work are formulated as follows:

- configuration of a normalised SIR-based projection system that projects (u, y) onto \mathcal{I}_Σ . The work will be performed in the framework of Hamiltonian systems and their dual form as a Legendre transform.
- introduction of a Bregman divergence induced by a Hamiltonian function and computation solution of the Bregman divergence from (u, y) to its projection. This solution will serve as an evaluation function for the detection (decision) logic.
- study on interpretations of the SIR-based projection and Bregman divergence as a fault detection system. Hereby, two aspects are of special interests: (i) the control theoretic insight, i.e. understanding of the Hamiltonian function induced Bregman divergence in the context of system performance-oriented fault detection, (ii) the interpretation from the viewpoint of information geometry and in the context of the projection theorem.
- discussion on the realisation and implementation issues. In order to achieve a reliable fault detection, it is of considerable practical importance to reduce false alarms. To this end, the defined Bregman divergence will be evaluated over an evaluation time interval. Moreover, a threshold should be set to ensure an optimal fault detection

decision. At the end of this work, a one-class fault detection scheme for nonlinear dynamic systems is completed.

- investigation on a scheme of a normalised SKR-based projection system. Although this work is analogue to the one of the SIR-based projection and fault detection system, it is significantly different in (i) its construction as an observer-based residual generator, (ii) the definition of the Bregman divergence, and in particular (iii) the interpretation of the Bregman divergence as a distance measure of (u, y) and the nominal system dynamics.
- study on the SKR-based projection system as an estimator for the uncertainty corrupted in (u, y) with a focus on (i) definition of an uncertainty model that should be independent of the possible types of uncertainties in the system, including faults, and thus lays the basis for interpreting and evaluating the estimation performance, (ii) evaluation of the projection-based estimation.

3 A projection and Bregman divergence based fault detection scheme

In this section, the first part of our work is presented. It is a projection-based scheme for detecting faults in the affine system (13). To be specific, a projection of process data (u, y) onto the image subspace \mathcal{I}_Σ is realised using the normalised SIR $\Sigma_{\mathcal{I}}$. Then, the introduction of a Hamiltonian function induced Bregman divergence and the associated Riemannian structure of the data manifold enables the definition and computation of a geodesic projection onto \mathcal{I}_Σ . Based on these theoretical results, fault detection algorithms are presented. To this end, we will first study the normalised SIR and its properties in the framework of Hamiltonian systems. It is followed by defining and analysing a Bregman divergence with the Hamiltonian function as a generating function. The proof that the normalised SIR-based projection is the geodesic projection gives an interesting interpretation of the projection as an important result of this study. At the end of this section, implementation issues towards a practical fault detection and the associated algorithm are discussed.

3.1 Normalised SIR and the associated Hamiltonian projection systems

Consider the affine system (13) and its SIR $\Sigma_{\mathcal{I}}$ given by (14). The corresponding Hamiltonian extension of $\Sigma_{\mathcal{I}}$ is the dynamic system described by

$$\begin{cases} \dot{x} = a_I(x) + B_I(x)v \\ \dot{\lambda} = - \left(\frac{\partial a_I(x)}{\partial x} + \frac{\partial B_I(x)}{\partial x} v \right)^T \lambda - \left(\frac{\partial c_I(x)}{\partial x} + \frac{\partial D_I(x)}{\partial x} v \right)^T v_a \\ \hat{z} = c_I(x) + D_I(x)v \in \mathbb{R}^{m+p} \\ z_a := B_I^T(x)\lambda + D_I^T(x)v_a \in \mathbb{R}^p. \end{cases}$$

For our purpose of projecting (u, y) onto the image subspace \mathcal{I}_Σ , connect v and z_a , i.e.

$$v = z_a = B_I^T(x)\lambda + D_I^T(x)v_a, \quad (42)$$

and let the data (u, y) be the input and \hat{z} the output of $\Sigma_{\mathcal{I}} \circ (D\Sigma_{\mathcal{I}})^T$,

$$v_a = \begin{bmatrix} u \\ y \end{bmatrix} =: z, \hat{z} = \Sigma_{\mathcal{I}} \circ (D\Sigma_{\mathcal{I}})^T(z).$$

Then, we have

$$\Sigma_{\mathcal{I}} \circ (D\Sigma_{\mathcal{I}})^T : \begin{cases} \dot{x} = a_I(x) + B_I(x)B_I^T(x)\lambda + B_I(x)D_I^T(x)z \\ \dot{\lambda} = - \left(\frac{\partial a_I(x)}{\partial x} + \frac{\partial \bar{B}_I(x, \lambda, z)}{\partial x} \right)^T \lambda - \left(\frac{\partial (c_I(x) + \bar{D}_I(x, \lambda, z))}{\partial x} \right)^T z \\ \hat{z} = c_I(x) + D_I(x)B_I^T(x)\lambda + D_I(x)D_I^T(x)z, \\ \bar{B}_I(x, \lambda, z) = B_I(x)B_I^T(x)\lambda + B_I(x)D_I^T(x)z, \\ \bar{D}_I(x, \lambda, z) = D_I(x)B_I^T(x)\lambda + D_I(x)D_I^T(x)z. \end{cases} \quad (43)$$

The configuration of $\Sigma_{\mathcal{I}} \circ (D\Sigma_{\mathcal{I}})^T$ is schematically depicted in Figure 1.

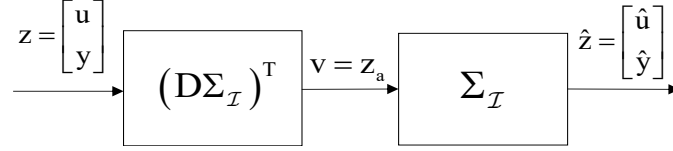


Figure 1: SIR-based projection system $\Sigma_{\mathcal{I}} \circ (D\Sigma_{\mathcal{I}})^T$

Define the Hamiltonian function

$$H(x, \lambda, z) = \frac{1}{2}z^T D_I(x)D_I^T(x)z + c_I^T(x)z + \lambda^T \left(a_I(x) + \frac{1}{2}B_I(x)B_I^T(x)\lambda + B_I(x)D_I^T(x)z \right). \quad (44)$$

It is straightforward that the Hamiltonian system (43) can then be written in the compact form

$$\Sigma_{\mathcal{I}} \circ (D\Sigma_{\mathcal{I}})^T : \begin{cases} \dot{x} = \frac{\partial H}{\partial \lambda}(x, \lambda, z) \\ \dot{\lambda} = -\frac{\partial H}{\partial x}(x, \lambda, z) \\ \hat{z} = \frac{\partial H}{\partial z}(x, \lambda, z). \end{cases} \quad (45)$$

Notice that the Hamiltonian function (44) can be, after some calculations, written as

$$\begin{aligned} H(x, \lambda, z) &= -\frac{1}{2}z^T D_I(x)D_I^T(x)z + \hat{z}^T z + \lambda^T \left(a_I(x) + \frac{1}{2}B_I(x)B_I^T(x)\lambda \right) \\ &= -\frac{1}{2}v^T v + \hat{z}^T z + \lambda^T \dot{x}, \\ \dot{x} &= a_I(x) + B_I(x)B_I^T(x)\lambda + B_I(x)D_I^T(x)z. \end{aligned} \quad (46)$$

Let

$$H^\times(x, \lambda, \hat{z}) = \hat{z}^T z - H(x, \lambda, z) = \frac{1}{2}v^T v - \lambda^T \dot{x}. \quad (47)$$

Note that

$$z = \frac{\partial H^\times(x, \lambda, \hat{z})}{\partial \hat{z}},$$

and the Hamiltonian system (45) can be expressed in terms of $H^\times(x, \lambda, \hat{z})$ as

$$\begin{cases} \dot{x} = -\frac{\partial H^\times}{\partial \lambda}(x, \lambda, \hat{z}) \\ \dot{\lambda} = \frac{\partial H^\times}{\partial x}(x, \lambda, \hat{z}) \\ z = \frac{\partial H^\times}{\partial \hat{z}}(x, \lambda, \hat{z}) \end{cases} \quad (48)$$

with \hat{z} as the input and z as the output. The above Hamiltonian system (48) has been investigated in the context of inner-outer factorisation and can be interpreted as the inverse of $-\Sigma_{\mathcal{I}} \circ (D\Sigma_{\mathcal{I}})^T$ and $H^\times(x, \lambda, \hat{z})$ as the Legendre dual of $H(x, \lambda, z)$ (Ball and van der Schaft, 1996). In other words, the Hamiltonian functions $H(x, \lambda, z)$ and $H^\times(x, \lambda, \hat{z})$ with

$$\hat{z} = \frac{\partial H}{\partial z}(x, \lambda, z) =: z^\times, \quad z = \frac{\partial H^\times}{\partial \hat{z}}(x, \lambda, \hat{z}),$$

form a Legendre transform and give the system data a dualistic structure. Here, \hat{z} is dual to z and thus is also denoted by z^\times . It is obvious from (46) that

$$H^\times(x, \lambda, z^\times) = \frac{1}{2}v^T v - \lambda^T \dot{x} = \frac{1}{2}z^T D_I(x) D_I^T(x) z - \lambda^T \left(a_I(x) + \frac{1}{2} B_I(x) B_I^T(x) \lambda \right). \quad (49)$$

Now, consider the normalised SIR and the corresponding Hamiltonian systems (45) and (48). The following theorem showcases that $\Sigma_{\mathcal{I}} \circ (D\Sigma_{\mathcal{I}})^T$ is an idempotent operator and the normalised SIR projects the process data (u, y) to \mathcal{I}_Σ .

Theorem 3 *Given the normalised SIR and the corresponding Hamiltonian system (43), then $\Sigma_{\mathcal{I}} \circ (D\Sigma_{\mathcal{I}})^T$ is idempotent, and*

$$\forall z = \begin{bmatrix} u \\ y \end{bmatrix} \in \mathcal{L}_2, \hat{z} \in \mathcal{I}_\Sigma, \quad (50)$$

$$\forall z \neq 0, \hat{z} = \begin{bmatrix} u \\ y \end{bmatrix} \text{ iff } \begin{bmatrix} u \\ y \end{bmatrix} \in \mathcal{I}_\Sigma. \quad (51)$$

Proof. That $\Sigma_{\mathcal{I}} \circ (D\Sigma_{\mathcal{I}})^T$ is idempotent immediately follows from the normalised SIR, i.e.

$$\Sigma_{\mathcal{I}} \circ (D\Sigma_{\mathcal{I}})^T \circ \Sigma_{\mathcal{I}} \circ (D\Sigma_{\mathcal{I}})^T = \Sigma_{\mathcal{I}} \circ (D\Sigma_{\mathcal{I}})^T.$$

The proof of (50) is apparent, since

$$(D\Sigma_{\mathcal{I}})^T \left(\begin{bmatrix} u \\ y \end{bmatrix} \right) =: v \in \mathcal{L}_2 \implies \Sigma_{\mathcal{I}} \circ (D\Sigma_{\mathcal{I}})^T \left(\begin{bmatrix} u \\ y \end{bmatrix} \right) = \Sigma_{\mathcal{I}}(v) \in \mathcal{I}_\Sigma.$$

To prove (51), observe that

$$\begin{aligned} \forall \begin{bmatrix} u \\ y \end{bmatrix} \in \mathcal{I}_\Sigma, \exists v \in \mathcal{L}_2, \text{ s.t. } \begin{bmatrix} u \\ y \end{bmatrix} = \Sigma_{\mathcal{I}}(v) \implies \\ \Sigma_{\mathcal{I}} \circ (D\Sigma_{\mathcal{I}})^T \left(\begin{bmatrix} u \\ y \end{bmatrix} \right) = \Sigma_{\mathcal{I}} \circ (D\Sigma_{\mathcal{I}})^T \circ \Sigma_{\mathcal{I}}(v) = \Sigma_{\mathcal{I}}(v) = \begin{bmatrix} u \\ y \end{bmatrix}. \end{aligned}$$

On the other hand, it follows from (50) that

$$\hat{z} = \begin{bmatrix} u \\ y \end{bmatrix} \implies \begin{bmatrix} u \\ y \end{bmatrix} \in \mathcal{I}_\Sigma.$$

Thus, (51) is proved. ■

Remark 3 That $\Sigma_{\mathcal{I}} \circ (D\Sigma_{\mathcal{I}})^T$ is idempotent is an important property that ensures the projection preserving local neighbourhoods at every point of the underlying manifold.

As a projection of (u, y) to \mathcal{I}_{Σ} , \hat{z} can be interpreted as an estimate of (u, y) as well. In this context, the notation

$$\hat{z} = \begin{bmatrix} \hat{u} \\ \hat{y} \end{bmatrix}$$

will also be adopted in the sequel.

Next, we consider the Hamiltonian functions (44) and (49) in case of the normalised SIR. It follows from Lemma 1 that for the normalised SIR,

$$P_x^T(x) a_I(x) + \frac{1}{2} c_I^T(x) c_I(x) = 0, P_x^T(x) B_I(x) + c_I^T(x) D_I(x) = 0, D_I^T(x) D_I(x) = I,$$

which yields

$$\begin{aligned} & \frac{1}{2} (c_I(x) + D_I(x) B_I^T(x) P_x(x))^T (c_I(x) + D_I(x) B_I^T(x) P_x(x)) \\ & \quad + P_x^T(x) \left(a_I(x) + \frac{1}{2} B_I(x) B_I^T(x) P_x(x) \right) = \\ P_x^T(x) a_I(x) + \frac{1}{2} c_I^T(x) c_I(x) + P_x^T(x) B_I(x) B_I^T(x) P_x(x) + c_I^T(x) D_I(x) B_I^T(x) P_x(x) &= 0. \end{aligned}$$

Hence, it holds

$$\begin{aligned} & P_x^T(x) \left(a_I(x) + \frac{1}{2} B_I(x) B_I^T(x) \lambda \right) - \frac{1}{2} z^T D_I(x) D_I^T(x) z \\ &= -\frac{1}{2} (c_I(x) + D_I(x) B_I^T(x) P_x(x))^T (c_I(x) + D_I(x) B_I^T(x) P_x(x)) - \frac{1}{2} z^T D_I(x) D_I^T(x) z \\ &= -\frac{1}{2} (\hat{z} - D_I(x) D_I^T(x) z)^T (\hat{z} - D_I(x) D_I^T(x) z) - \frac{1}{2} z^T D_I(x) D_I^T(x) z \\ &= -\frac{1}{2} \hat{z}^T \hat{z} + \hat{z}^T D_I(x) D_I^T(x) z - \frac{1}{2} z^T D_I(x) D_I^T(x) z. \end{aligned} \tag{52}$$

In the course of this computation we have used the relations

$$\begin{aligned} \hat{z} &= c_I(x) + D_I(x) B_I^T(x) P_x(x) + D_I(x) D_I^T(x) z, \\ D_I(x) D_I^T(x) D_I(x) D_I^T(x) &= D_I(x) D_I^T(x). \end{aligned}$$

By (46), (49) and (52), the following theorem is apparent.

Theorem 4 Given the normalised SIR and the corresponding Hamiltonian system (43), then

$$H^\times(x, \lambda, z^\times) = \frac{1}{2} \hat{z}^T \hat{z}, \tag{53}$$

$$H(x, \lambda, z) = \hat{z}^T z - \frac{1}{2} \hat{z}^T \hat{z}. \tag{54}$$

Proof. It is apparent that we have, according to (46), (49) and (52),

$$\begin{aligned} H^\times(x, \lambda, z^\times) &= \frac{1}{2} \hat{z}^T \hat{z} - \hat{z}^T D_I(x) D_I^T(x) z + z^T D_I(x) D_I^T(x) z, \\ H(x, \lambda, z) &= \hat{z}^T (I + D_I(x) D_I^T(x)) z - \frac{1}{2} \hat{z}^T \hat{z} - z^T D_I(x) D_I^T(x) z. \end{aligned}$$

Notice that

$$\begin{aligned} \hat{z}^T D_I(x) D_I^T(x) z &= (c_I(x) + D_I(x) B_I^T(x) P_x(x) + D_I(x) D_I^T(x) z)^T D_I(x) D_I^T(x) z \\ &= (c_I^T(x) D_I(x) + P_x^T(x) B_I(x)) D_I^T(x) z + z^T D_I(x) D_I^T(x) z \\ &= z^T D_I(x) D_I^T(x) z. \end{aligned}$$

Hence,

$$H^\times(x, \lambda, z^\times) = \frac{1}{2} \hat{z}^T \hat{z}, \quad H(x, \lambda, z) = \hat{z}^T z - \frac{1}{2} \hat{z}^T \hat{z}.$$

■

An immediate result of Theorems 3 and 4 is the following corollary, which is useful for us to examine the interpretation of the both Hamiltonian functions as generalised energy functions and, based on it, to establish our fault detection strategy.

Corollary 1 *Given the normalised SIR and the corresponding Hamiltonian system (43), then*

$$\forall \begin{bmatrix} u \\ y \end{bmatrix} \in \mathcal{I}_\Sigma, \quad H^\times(x, \lambda, z^\times) = H(x, \lambda, z) = \frac{1}{2} \hat{z}^T \hat{z} = \frac{1}{2} z^T z = \frac{1}{2} v^T v - \dot{P}(x),$$

where $P(x) \geq 0$ is the solution of the HJE (34).

Proof. It follows from Theorem 3 that

$$\forall \begin{bmatrix} u \\ y \end{bmatrix} \in \mathcal{I}_\Sigma, \quad \hat{z} = \Sigma_{\mathcal{I}} \circ (D\Sigma_{\mathcal{I}})^T(z) = z.$$

Thus, according to Theorem 4 that

$$H^\times(x, \lambda, z^\times) = H(x, \lambda, z) = \frac{1}{2} \hat{z}^T \hat{z} = \frac{1}{2} z^T z.$$

On the other hand, for the normalised SIR,

$$\lambda = P_x(x) \implies \lambda^T \dot{x} = \dot{P}(x),$$

which leads to

$$\begin{aligned} H(x, \lambda, z) &= \hat{z}^T z - \frac{1}{2} v^T v + \dot{P}(x) = H^\times(x, \lambda, z^\times) = \frac{1}{2} v^T v - \dot{P}(x) \\ \implies \hat{z}^T z &= z^T z = v^T v - 2\dot{P}(x) \implies H(x, \lambda, z) = H^\times(x, \lambda, z^\times) = \frac{1}{2} v^T v - \dot{P}(x). \end{aligned}$$

The theorem is proved. ■

Corollary 1 tells us, corresponding to the nominal system dynamics, both Hamiltonian functions (44) and (47) as energy functions are equivalent. Moreover, from the viewpoint of the

energy balance, the lossless property, as defined in Definition 2 and in the sense of (27), holds. When uncertainties or faults are present in the system, i.e. $z \notin \mathcal{I}_\Sigma$, such an energy balance will be disturbed, as described by (54) in Theorem 4. In this context, the fault detection problem can be formulated as detecting deviations of the Hamiltonian functions from the nominal value $\frac{1}{2}\hat{z}^T\hat{z} = \frac{1}{2}z^Tz$. To this end, it is plain that a well-founded evaluation function should be defined in such a way that it is possible to examine the energy balance relations real-time and thus to detect possible changes in the parity relations reliably and timely. This is the problem to be addressed in the next subsection.

3.2 A Bregman divergence-based evaluation function, and geodesic projection

In the well-established observer-based fault detection framework, building (i) a residual vector as the difference between the measurement and its estimate, (ii) evaluating the residual vector by means of a signal norm, typically \mathcal{L}_2 norm, are the two essential steps to a successful fault detection. In our divergence-based detection framework, we propose, alternatively, to evaluate possible changes in the system dynamic in terms of a divergence between the measurement (data) and its estimate (projection). The basic idea behind this approach is twofold, as motivated and described in the section of problem formulation,

- to achieve a system performance-oriented fault detection by means of a Hamiltonian function induced Bregman divergence, and
- to detect deviations using a Bregman divergence as a distance measure.

Consider the normalised SIR (14) and the corresponding Hamiltonian system (43) with the input and output vectors, z and \hat{z} , where z is the collected data and \hat{z} is its estimate (projection) delivered by (43). In the sequel, for the sake of notation simplicity, the Hamiltonian functions (44) and (49) are expressed respectively by

$$H(z) := H(x, \lambda, z), H^\times(z) := H^\times(x, \lambda, z).$$

Since our objective is to detect faults by checking deviations from the nominal dynamics, we examine, according to Corollary 1, the condition

$$H^\times(z) = H(z) = \frac{1}{2}\hat{z}^T\hat{z} = \frac{1}{2}z^Tz. \quad (55)$$

To this end, the following hypothesis test is under consideration:

$$\begin{cases} \mathcal{H}_0 : H^\times(z) = H(z) = \frac{1}{2}\hat{z}^T\hat{z} = \frac{1}{2}z^Tz \\ \mathcal{H}_1 : H(z) \neq \frac{1}{2}z^Tz. \end{cases} \quad (56)$$

Here, the hypothesis \mathcal{H}_0 represents the nominal dynamics, while \mathcal{H}_1 indicates faulty dynamics. Let the Bregman divergence

$$D_{H_0}[\hat{z} : z] := H_0(\hat{z}) - H_0(z) - \left(\frac{\partial H_0(z)}{\partial z} \right)^T (\hat{z} - z),$$

be the test (evaluation) function for the implementation of the hypothesis test (56), where $H_0(z)$ represents the nominal dynamics and thus is subject to

$$H_0(z) = \frac{1}{2}z^T z.$$

The computation of $D_{H_0} [\hat{z} : z]$ is given in following theorem, which also provides us with an interesting interpretation of $D_{H_0} [\hat{z} : z]$.

Theorem 5 *Given the normalised SIR (14), the corresponding Hamiltonian system (43) and Hamiltonian functions (44) and (49), then the Bregman divergence*

$$D_{H_0} [\hat{z} : z] = H_0(\hat{z}) - H_0(z) - \left(\frac{\partial H_0(z)}{\partial z} \right)^T (\hat{z} - z)$$

is given by

$$D_{H_0} [\hat{z} : z] = H_0(z) - H(z), \quad (57)$$

$$H(z) = \hat{z}^T z - \frac{1}{2}\hat{z}^T \hat{z}. \quad (58)$$

Proof. Recall that z and \hat{z} are a Legendre dual pair,

$$\hat{z} = \frac{\partial H(x, \lambda, z)}{\partial z} = z^\times, \quad z = \frac{\partial H^\times(x, \lambda, \hat{z})}{\partial \hat{z}}.$$

Hence, according to Corollary 1, (54) in Theorem 4 and (40), we have

$$\begin{aligned} D_{H_0} [\hat{z} : z] &= H_0(\hat{z}) + H_0(z) - z^T \hat{z} = H_0(z) - H(z), \\ H_0(z) &= \frac{1}{2}z^T z, \quad H(z) = z^T \hat{z} - H_0(\hat{z}) = \hat{z}^T z - \frac{1}{2}\hat{z}^T \hat{z}. \end{aligned}$$

■

Theorem 5 demonstrates that the Bregman divergence $D_{H_0} [\hat{z} : z]$ gives a distance measure between process data z and its projection on to $\mathcal{I}_\Sigma, \hat{z}$, in terms of the deviation of the Hamiltonian function from its nominal value $H_0(z)$, expressed by $H_0(z) - H(z)$.

We would like to draw the reader's attention to the fact that

$$D_{H_0} [\hat{z} : z] = \frac{1}{2}z^T z + \frac{1}{2}\hat{z}^T \hat{z} - \hat{z}^T z = \frac{1}{2}\|z - \hat{z}\|^2,$$

i.e. $D_{H_0} [\hat{z} : z]$ is one half of the squared Euclidean norm of the projection-based residual $z - \hat{z}$. Although, due to the generating function defined by $H_0(z) = \frac{1}{2}z^T z$, this is a known mathematical result, the underlined control-theoretic interpretation is of remarkable importance. That is, the squared Euclidean norm of the projection-based residual gives the deviation of the Hamiltonian function from its nominal value. In other words, the norm-based evaluation of the projection-based residual implies a performance-oriented evaluation and thus leads to a performance-oriented fault detection. This property marks a distinguishing difference of the proposed detection scheme to the well-established model- and observer-based fault detection framework.

It is worth emphasising that in a non-Euclidean space, the relation with the above orthogonal projection as given in (12) does not hold. Our intention of introducing the Bregman divergence as a distance measure is to find an alternative solution. In this regard, it is of considerable theoretic interest to study the projection $\hat{z} = \Sigma_{\mathcal{I}} \circ (D\Sigma_{\mathcal{I}})^T(z)$ from the viewpoint of information geometry. To this end, the projection theorem (Amari, 2016) is applied.

Consider the Bregman divergence from the process data z to the system image manifold \mathcal{I}_{Σ} derived by $D_{H^{\times}}$,

$$D_{H^{\times}}[z : \mathcal{I}_{\Sigma}] = \min_{z_0 \in \mathcal{I}_{\Sigma}} D_{H^{\times}}[z : z_0]. \quad (59)$$

The following theorem provides us with the interpretation that the projection \hat{z} delivered by the Hamiltonian system (43) is a geodesic projection.

Theorem 6 *Consider the normalised SIR (14) and the Bregman divergence $D_{H^{\times}}[z : \mathcal{I}_{\Sigma}]$. The projection \hat{z} delivered by the corresponding Hamiltonian system (43) is a geodesic projection of z onto \mathcal{I}_{Σ} . Moreover, the Bregman divergence $D_{H^{\times}}[z : \mathcal{I}_{\Sigma}]$ is given by*

$$D_{H^{\times}}[z : \mathcal{I}_{\Sigma}] = \frac{1}{2}z^T z + \frac{1}{2}\hat{z}^T \hat{z} - z^T \hat{z}. \quad (60)$$

Proof. It follows from Theorem 2 that the geodesic projection of z onto \mathcal{I}_{Σ} is the vector z^* that minimises $D_{H^{\times}}[z : z_0], \forall z_0 \in \mathcal{I}_{\Sigma}$, i.e.

$$D_{H^{\times}}[z : \mathcal{I}_{\Sigma}] = \min_{z_0 \in \mathcal{I}_{\Sigma}} D_{H^{\times}}[z : z_0] = D_{H^{\times}}[z : z^*].$$

Accordingly, it is to prove

$$\hat{z} = z^* = \arg \min_{z_0 \in \mathcal{I}_{\Sigma}} D_{H^{\times}}[z : z_0]. \quad (61)$$

To this end, consider, following (40) and noticing $\forall z_0 \in \mathcal{I}_{\Sigma}, z_0^{\times} = \hat{z}_0 = z_0$,

$$D_{H^{\times}}[z : z_0] = H^{\times}(z) + H(z_0^{\times}) - z^T z_0^{\times} = H^{\times}(z) + H(z_0) - z^T z_0.$$

It yields, by Theorems 3 and 4,

$$H(z_0) = \frac{1}{2}z_0^T z_0 \implies D_{H^{\times}}[z : z_0] = \frac{1}{2}z^T z + \frac{1}{2}z_0^T z_0 - z^T z_0. \quad (62)$$

Hence, the optimisation problem becomes

$$\min_{z_0 \in \mathcal{I}_{\Sigma}} \left(\frac{1}{2}z_0^T z_0 - z^T z_0 \right).$$

Recall that $\forall z_0 \in \mathcal{I}_{\Sigma}$

$$D_I(x)D_I^T(x)z_0 + c_I(x) + D_I(x)B_I^T(x)P_x(x) = z_0, \quad (63)$$

$$D_I^T(x)D_I(x) = I, (c_I(x) + D_I(x)B_I^T(x)P_x(x))^T D_I(x) = 0, \quad (64)$$

which yields

$$\begin{aligned} z_0^T z_0 &= z_0^T D_I(x)D_I^T(x)z_0 + (c_I(x) + D_I(x)B_I^T(x)P_x(x))^T (c_I(x) + D_I(x)B_I^T(x)P_x(x)), \\ z^T z_0 &= z^T (c_I(x) + D_I(x)B_I^T(x)P_x(x) + D_I(x)D_I^T(x)z_0). \end{aligned}$$

Thus, it holds

$$\min_{z_0 \in \mathcal{I}_\Sigma} \left(\frac{1}{2} z_0^T z_0 - z^T z_0 \right) \iff \min_{z_0 \in \mathcal{I}_\Sigma} \left(\frac{1}{2} z_0^T D_I(x) D_I^T(x) z_0 - z^T D_I(x) D_I^T(x) z_0 \right).$$

Solving

$$\frac{\partial}{\partial z_0} \left(\frac{1}{2} z_0^T D_I(x) D_I^T(x) z_0 - z^T D_I(x) D_I^T(x) z_0 \right) = 0$$

gives

$$D_I(x) D_I^T(x) z^* = D_I(x) D_I^T(x) z, \quad (65)$$

where z^* represents the optimal solution that belongs to \mathcal{I}_Σ . It is known that

$$\hat{z} = c_I(x) + D_I(x) B_I^T(x) P_x(x) + D_I(x) D_I^T(x) z \in \mathcal{I}_\Sigma.$$

It follows immediately from (63)-(64) that

$$z^* = \hat{z}$$

solves (65). Finally, substituting z_0 in (62) by \hat{z} leads to (60). The theorem is proved. ■

This result gives a nice interpretation of the projection $\hat{z} = \Sigma_{\mathcal{I}} \circ (D\Sigma_{\mathcal{I}})^T(z)$. Thanks to the Bregman divergence D_{H^\times} and the Legendre transform, the data manifold is equipped with a dual Riemannian structure and dually flat (Amari, 2016). In this context, the projection \hat{z} is a geodesic projection of z onto \mathcal{I}_Σ , and the distance defined by the Bregman divergence D_{H^\times} is at minimum. This result can be interpreted as a generalisation of the orthogonal projection (9) defined in Hilbert space.

As a summary of this subsection, it is concluded that the two major objectives of our work, (i) system performance-oriented fault detection by means of a Hamiltonian function induced Bregman divergence, (ii) detection of deviations in a non-Euclidean space using a Bregman divergence as a distance measure, have been satisfactorily achieved.

3.3 Implementation issues

Before the theoretical results presented in the previous subsections can be applied to a reliable fault detection, two fault detection specified issues should be clarified. They are,

- definition of a reliable (robust) evaluation function J and, based on it,
- determination of a threshold J_{th} .

The first issue is of considerable importance to reduce false alarms. For instance, the Bregman divergence $D_{H_0}[\hat{z} : z]$ given in (57) is a time function. When it is directly used as an evaluation function, detection decision will be made solely depending on the data received at a single time instant. Due to possible transient disturbances during system operations, such handling would probably result in a flood of false alarms. Concerning the second issue, it is natural that, under the detection logic,

$$\text{detection logic: } \begin{cases} J \leq J_{th} \implies \text{fault-free} \\ J > J_{th} \implies \text{faulty,} \end{cases}$$

the selection of J_{th} would have a crucial influence on the detection performance. An integrated design of (J, J_{th}) is state of the art in model-based fault detection towards an optimal trade-off between the false alarm rate and fault detection rate (Ding, 2008; Ding, 2020). Below, these two issues are addressed jointly.

Let $[t_0, t_1]$ be the evaluation time window and define

$$J = \int_{t_0}^{t_1} D_{H_0} [\hat{z} : z] d\tau = \int_{t_0}^{t_1} \left(H_0(\hat{z}) - H_0(z) - \left(\frac{\partial H_0(z)}{\partial z} \right)^T (\hat{z} - z) \right) d\tau \quad (66)$$

as the evaluation function. In the literature, the divergence given by (66) is called pointwise Bregman divergence (Frigyik *et al.*, 2008). Consider that, in real applications, digital data are collected and recorded. Suppose that over the time interval $[t_0, t_1]$, $z(k_i)$, $i = 1, \dots, M$, are collected, where k_i denotes the sampling instant. For our purpose of fault detection, an approximation of function (66) is implemented using the available data $z(k_i)$ as follows,

$$\begin{aligned} J &= \frac{1}{M} \sum_{i=1}^M D_{H_0} [\hat{z}(k_i) : z(k_i)] \\ &= \frac{1}{M} \sum_{i=1}^M \left(H_0(\hat{z}(k_i)) - H_0(z(k_i)) - \left(\frac{\partial H_0(z(k_i))}{\partial z(k_i)} \right)^T (\hat{z}(k_i) - z(k_i)) \right) \\ &= \frac{1}{M} \sum_{i=1}^M (H_0(z(k_i)) - H_0(\hat{z}(k_i)) - z^T(k_i) \hat{z}(k_i)) \\ &= \frac{1}{M} \sum_{i=1}^M (H_0(z(k_i)) - H(\hat{z}(k_i))). \end{aligned} \quad (67)$$

It is of interest to note that the above evaluation function J is equivalent to the Bregman divergence defined by

$$D_{H_0} [\hat{z}_M : z_M] := H_{0,M}(\hat{z}_M) - H_{0,M}(z_M) - \left(\frac{\partial H_{0,M}(z_M)}{\partial z_M} \right)^T (\hat{z}_M - z_M), \quad (68)$$

$$H_{0,M}(z_M) := \frac{1}{M} \sum_{i=1}^M H_0(z(k_i)) = \frac{1}{2} z_M^T z_M, \quad H_{0,M}(\hat{z}_M) = \frac{1}{2} \hat{z}_M^T \hat{z}_M, \quad (69)$$

$$z_M := \begin{bmatrix} \frac{z(k_1)}{\sqrt{M}} \\ \vdots \\ \frac{z(k_M)}{\sqrt{M}} \end{bmatrix} \in \mathbb{R}^{M(m+p)}, \quad \hat{z}_M := \begin{bmatrix} \frac{\hat{z}(k_1)}{\sqrt{M}} \\ \vdots \\ \frac{\hat{z}(k_M)}{\sqrt{M}} \end{bmatrix} \in \mathbb{R}^{M(m+p)},$$

as proved in the following theorem.

Theorem 7 *Given the normalised SIR (14), the corresponding Hamiltonian system (43) and Hamiltonian function (49), and suppose that $z(k_i)$, $i = 1, \dots, M$, are available. Then, the evaluation function (67) is equivalent to the Bregman divergence (68) with the generating*

function (69) and can be written as

$$J = D_{H_0} [\hat{z}_M : z_M] = \frac{1}{2} z_M^T z_M + \frac{1}{2} \hat{z}_M^T \hat{z}_M - \hat{z}_M^T z_M \quad (70)$$

$$= H_{0,M}(z_M) - H_M(z_M), \quad (71)$$

$$H_M(z_M) = \frac{1}{M} \sum_{i=1}^M H(z(k_i)) = \frac{1}{M} \sum_{i=1}^M (\hat{z}^T(k_i) z(k_i) - H^\times(z(k_i))). \quad (72)$$

Proof. It is apparent that by definition

$$\begin{aligned} J &= \frac{1}{M} \sum_{i=1}^M \left(H_0(\hat{z}(k_i)) - H_0(z(k_i)) - \left(\frac{\partial H_0(z(k_i))}{\partial z(k_i)} \right)^T (\hat{z}(k_i) - z(k_i)) \right) \\ &= \frac{1}{2} z_M^T z_M + \frac{1}{2} \hat{z}_M^T \hat{z}_M - z_M^T (\hat{z}_M - z_M) \\ &= H_{0,M}(\hat{z}_M) - H_{0,M}(z_M) - \left(\frac{\partial H_{0,M}(z_M)}{\partial z_M} \right)^T (\hat{z}_M - z_M), \end{aligned}$$

which proves (70). Concerning (71) and (72), notice that (z_M, \hat{z}_M) builds a dual pair of Legendre transform with

$$z_M = \frac{\partial H_M^\times(\hat{z}_M)}{\partial \hat{z}_M} = \begin{bmatrix} \frac{\partial H^\times(\hat{z}(k_1))}{\partial \hat{z}(k_1)} \frac{1}{\sqrt{M}} \\ \vdots \\ \frac{\partial H^\times(\hat{z}(k_M))}{\partial \hat{z}(k_M)} \frac{1}{\sqrt{M}} \end{bmatrix} = \begin{bmatrix} \frac{z(k_1)}{\sqrt{M}} \\ \vdots \\ \frac{z(k_M)}{\sqrt{M}} \end{bmatrix}, \hat{z}_M = \frac{\partial H_M(z_M)}{\partial z_M}, \quad (73)$$

$$H_M(z_M) = \hat{z}_M^T z_M - H_M^\times(\hat{z}_M) = \frac{1}{M} \sum_{i=1}^M (\hat{z}^T(k_i) z(k_i) - H^\times(z(k_i))), \quad (74)$$

where

$$H_M^\times(\hat{z}_M) = \frac{1}{M} \sum_{i=1}^M H^\times(z(k_i)).$$

Consequently, the Bregman divergence (68) can be written as

$$D_{H_0} [\hat{z}_M : z_M] = H_{0,M}(z_M) + H_M^\times(\hat{z}_M) - z_M^T \hat{z}_M = H_{0,M}(z_M) - H_M(z_M)$$

Hence, (71) and (72) are proved. ■

Theorem 7 and its proof not only reveal that the evaluation function J is a Bregman divergence, but also pose the basis of a potential framework of data-driven fault detection. The centerpiece of this framework is the Bregman divergence $D_{H_0} [\hat{z}_M : z_M]$ and the Legendre transform (73)-(74), which would enable to endow the data set

$$\mathcal{M} = \left\{ \begin{bmatrix} z(k_1) \\ \vdots \\ z(k_M) \end{bmatrix} \in \mathcal{L}_2, z(k_i) = \begin{bmatrix} u(k_i) \\ y(k_i) \end{bmatrix}, i = 1, \dots, M \right\}$$

with a dual Riemannian structure and thus a projection-based fault detection. This issue is a part of our future work and will not be discussed in the draft.

Before introducing the threshold setting scheme, we would like to place a greater emphasis on the basic task of one-class fault detection. Simply speaking, it is to detect anomalies arising during normal system operations. The challenge is a reliable detection of those incipient anomalies as early as possible in spite of possibly existing uncertainties in the system. Now, we are in the position to study the threshold setting issue on the assumption of the evaluation function J given by (67).

Recall that the Bregman divergence $D_{H_0} [\hat{z}_M : z_M]$ gives the difference between the nominal Hamiltonian function $H_{0,M}(z_M)$ as a reference and the real Hamiltonian function $H_M(z_M)$ over the time interval $[t_0, t_1]$. During the ideal operation without faults and uncertainty,

$$z_M = \hat{z}_M, H_M^\times(z_M) = H_{0,M}(z_M) = \frac{1}{2} z_M^T z_M \implies J = D_{H_0} [\hat{z}_M : z_M] = 0.$$

The term $z_M^T \hat{z}_M$ describes the influence of anomalies and uncertainties causing $z_M \neq \hat{z}_M$. Since

$$\hat{z}_M = \frac{\partial H_M(z_M)}{\partial z_M}$$

gives the directional derivative of $H_M(z_M)$ in the direction z_M , it is at maximum, when the direction \hat{z}_M coincides with the gradient of $H_M(z_M)$. In other words, during the nominal operation, $H_M(z_M)$ is at maximum,

$$H_M(z_M) = \left(\frac{\partial H_M(z_M)}{\partial z_M} \right)^T z_M - \frac{1}{2} \left(\frac{\partial H_M(z_M)}{\partial z_M} \right)^T \frac{\partial H_M(z_M)}{\partial z_M} = \frac{1}{2} z_M^T z_M.$$

As uncertainties or faults emerge, it becomes smaller. Let $\gamma \in [0.5, 1]$ be the tolerant limit so that it is accepted as fault-free operation when

$$\gamma \leq \frac{H_M(z_M)}{\frac{1}{2} z_M^T z_M} = \frac{2\hat{z}_M^T z_M - \hat{z}_M^T \hat{z}_M}{z_M^T z_M}.$$

Accordingly, when

$$\frac{D_{H_0} [\hat{z}_M : z_M]}{\frac{1}{2} z_M^T z_M} = 1 - \frac{H_M(z_M)}{\frac{1}{2} z_M^T z_M} = 1 - \frac{2\hat{z}_M^T z_M - \hat{z}_M^T \hat{z}_M}{z_M^T z_M} \leq 1 - \gamma,$$

the system operation is identified as fault-free. In this context, the threshold is set to be

$$J_{th} = \frac{1}{2} (1 - \gamma) z_M^T z_M. \quad (75)$$

Here, γ is assumed to be known or determined from the real fault-free operation or simulation data, say e.g. $\gamma = 0.95$.

At the end of this section, the online detection algorithm is summarised as follows:

- Collection of data $z(k_i)$ and computation of $\hat{z}(k_i)$, $i = 1, \dots, M$, according to (45);
- Computation of the evaluation function J according to (70);
- Detection decision logic:

$$\begin{cases} J \leq J_{th} \implies \text{fault-free} \\ J > J_{th} \implies \text{faulty.} \end{cases}$$

4 An SKR-based fault detection scheme, and uncertainty/fault estimation

Thanks to the dual relation of SKR and SIR, most of the schemes and ideas of our study in this section on the application of the normalised SKR-based projection to fault detection are analogue to the ones presented in the previous section. Hence, our descriptions and discussions on the related issues will be shortened. On the other hand, intensive endeavours will be made to highlight the projection-based estimation of system uncertainties and faults aiming at insightfully understanding and interpreting the normalised SKR-based projection.

4.1 On the uncertainty corrupted in process data and its estimation

In this subsection, we take a closer look at system $(D\Sigma_{\mathcal{K}})^T \circ \Sigma_{\mathcal{K}}$ and delineate its use for estimating uncertainties/faults corrupted in the process data (u, y) . We begin with the Hamiltonian extension of $\Sigma_{\mathcal{K}}$,

$$\begin{cases} \dot{\hat{x}} = a_K(\hat{x}) + B_K(\hat{x})z, z := \begin{bmatrix} u \\ y \end{bmatrix} \\ \dot{\lambda} = - \left(\frac{\partial a_K(\hat{x})}{\partial \hat{x}} + \frac{\partial B_K(\hat{x})}{\partial \hat{x}} z \right)^T \lambda - \left(\frac{\partial c_K(\hat{x})}{\partial \hat{x}} + \frac{\partial D_K(\hat{x})}{\partial \hat{x}} z \right)^T z_a \\ r_y = c_K(\hat{x}) + D_K(\hat{x})z \\ r_{y,a} = B_K^T(\hat{x})\lambda + D_K^T(\hat{x})z_a, z_a \in \mathbb{R}^m, r_{y,a} \in \mathbb{R}^{m+p}. \end{cases} \quad (76)$$

Connecting r_y and z_a , and defining the Hamiltonian function,

$$H(\hat{x}, \lambda, z) = \frac{1}{2} (c_K(\hat{x}) + D_K(\hat{x})z)^T (c_K(\hat{x}) + D_K(\hat{x})z) + \lambda^T (a_K(\hat{x}) + B_K(\hat{x})z), \quad (77)$$

give the Hamiltonian system $(D\Sigma_{\mathcal{K}})^T \circ \Sigma_{\mathcal{K}}$,

$$(D\Sigma_{\mathcal{K}})^T \circ \Sigma_{\mathcal{K}} : \begin{cases} \dot{\hat{x}} = \frac{\partial H(\hat{x}, \lambda, z)}{\partial \lambda} \\ \dot{\lambda} = - \frac{\partial H(\hat{x}, \lambda, z)}{\partial \hat{x}} \\ r_{y,a} = \frac{\partial H(\hat{x}, \lambda, z)}{\partial z}. \end{cases} \quad (78)$$

System $(D\Sigma_{\mathcal{K}})^T \circ \Sigma_{\mathcal{K}}$ is an $\mathcal{L}_2 \rightarrow \mathcal{L}_2$ mapping which can be interpreted as an estimation of the uncertainty corrupted in the data z , as will be discussed in the sequel. For this reason, we adopt the notation

$$\hat{z}_{\Delta} := r_{y,a} = (D\Sigma_{\mathcal{K}})^T \circ \Sigma_{\mathcal{K}}(z).$$

Figure 2 sketches the configuration of $(D\Sigma_{\mathcal{K}})^T \circ \Sigma_{\mathcal{K}}$ schematically.

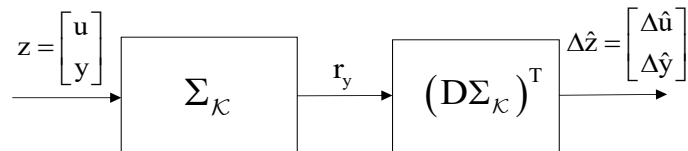


Figure 2: SKR-based projection system $(D\Sigma_{\mathcal{K}})^T \circ \Sigma_{\mathcal{K}}$

4.1.1 Co-inner and uncertainties

Recall that the normalised SKR is a co-inner. That means, by definition, the system

$$r_y = \Sigma_{\mathcal{K}} \circ (D\Sigma_{\mathcal{K}})^T(z_a),$$

configured by connecting z and $r_{y,a}$ in the Hamiltonian extension of $\Sigma_{\mathcal{K}}$ (76), is of the lossless property, namely,

$$\begin{aligned} r_y &= z_a, \\ \exists V(x) \geq 0, V(0) = 0, \text{ s.t. } V(x(t_2)) - V(x(t_1)) &= \frac{1}{2} \int_{t_1}^{t_2} (r_{y,a}^T r_{y,a} - r_y^T r_y) d\tau. \end{aligned}$$

It leads to

$$r_{y,a} = (D\Sigma_{\mathcal{K}})^T(z_a) = (D\Sigma_{\mathcal{K}})^T(r_y). \quad (79)$$

Since the residual vector r_y contains informations about uncertainties in the system, relation (79) indicates that the output of the system $(D\Sigma_{\mathcal{K}})^T(r_y)$ is of the character of uncertainties. This observation draws our attention on the (normalised) SKR and system uncertainties.

4.1.2 System kernel and uncertainty models

In advanced control and model-based fault diagnosis theories, handling of system uncertainties is an essential issue. There are numerous ways to model various types of model uncertainties and, based on them, the influences (often in form of an upper-bound) of system uncertainties on the system output or the residual signal can be estimated and used, e.g. for robust controller design (Francis, 1987; Vinnicombe, 2000; Zhou *et al.*, 1996; van der Schaft, 2000) or threshold setting in a fault detection scheme (Ding, 2008; Ding, 2020). Below, we introduce a model that describes uncertainties corrupted in the system data (u, y) . This model underlines the insightful interpretation of the projection $\hat{z}_{\Delta} = (D\Sigma_{\mathcal{K}})^T \circ \Sigma_{\mathcal{K}}(z)$ as an estimator for uncertainties/faults.

To begin with, a modified form of the SKR $\Sigma_{\mathcal{K}}$ (16),

$$\begin{cases} \dot{\hat{x}} = a_K(\hat{x}) + B_K(\hat{x}) \begin{bmatrix} u \\ y \end{bmatrix} \\ r_y = c_K(\hat{x}) + D_K(\hat{x}) \begin{bmatrix} u \\ y \end{bmatrix} \\ y = \hat{y} + W^{-1}(\hat{x})r_y, \hat{y} = c(\hat{x}) + D(\hat{x})u, \end{cases} \quad (80)$$

is introduced. Model (80) describes the I/O-dynamics of the system (13), and thus is called kernel-based I/O model. Apparently, it models the I/O dynamics both in the nominal and uncertain/faulty operations, and is independent of all possible types of system uncertainties. A plausible explanation of this distinguishing capability is the fact that system uncertainties are implicitly corrupted in the process data (u, y) and represented by the residual vector r_y . This raises the question of whether it is possible to (i) model the uncertainties corrupted in (u, y) , and (ii) estimate them. An apparent answer in case of a linear system, as shown below, motivates our work.

Example 1 *Let*

$$\begin{bmatrix} u \\ y \end{bmatrix} = \begin{bmatrix} u_0 \\ y_0 \end{bmatrix} + \begin{bmatrix} \Delta u \\ \Delta y \end{bmatrix}, \quad (81)$$

where $\begin{bmatrix} u_0 \\ y_0 \end{bmatrix} \in \mathcal{I}_\Sigma$ denotes the nominal operation, and $\begin{bmatrix} \Delta u \\ \Delta y \end{bmatrix}$ represents the uncertainties, for instance, caused by unknown input vectors in the system. As described in Section 2.1, we have

$$\begin{cases} \dot{\hat{x}} = A_L \hat{x} + \begin{bmatrix} B_L & -L \end{bmatrix} \begin{bmatrix} u \\ y \end{bmatrix} \\ r_y = -W \left(C \hat{x} + \begin{bmatrix} -D & I \end{bmatrix} \begin{bmatrix} u \\ y \end{bmatrix} \right) \end{cases} = \begin{cases} \dot{\hat{x}}_\Delta = A_L \hat{x}_\Delta + \begin{bmatrix} B_L & -L \end{bmatrix} \begin{bmatrix} \Delta u \\ \Delta y \end{bmatrix} \\ r_y = -W \left(C \hat{x}_\Delta + \begin{bmatrix} -D & I \end{bmatrix} \begin{bmatrix} \Delta u \\ \Delta y \end{bmatrix} \right), \end{cases}$$

$$A_L = A - LC, B_L = B - LD,$$

since it holds $K_G I_G = 0$. Here, the state variables \hat{x} and \hat{x}_Δ are generally different, and the two systems are equal in the context that they deliver the identical output.

Although for nonlinear systems the data corrupted with uncertainties cannot be written in the additive form like (81), this example inspires the introduction of the following uncertainty model.

Definition 6 *Given the normalised SKR (16), the state space representation of $\Delta\Sigma_{\mathcal{K}}$,*

$$\Delta\Sigma_{\mathcal{K}} : \begin{cases} \dot{\hat{x}}_\Delta = a_K(\hat{x}_\Delta) + B_K(\hat{x}_\Delta) \begin{bmatrix} \Delta u \\ \Delta y \end{bmatrix} \\ r_y = c_K(\hat{x}_\Delta) + D_K(\hat{x}_\Delta) \begin{bmatrix} \Delta u \\ \Delta y \end{bmatrix}, \end{cases} \hat{x}_\Delta(0) = 0, \begin{bmatrix} \Delta u \\ \Delta y \end{bmatrix} =: \Delta z \in \mathcal{L}_2, \quad (82)$$

subject to

$$\begin{cases} \dot{\hat{x}}_\Delta = a_K(\hat{x}_\Delta) + B_K(\hat{x}_\Delta) \begin{bmatrix} \Delta u \\ \Delta y \end{bmatrix} \\ r_y = c_K(\hat{x}_\Delta) + D_K(\hat{x}_\Delta) \begin{bmatrix} \Delta u \\ \Delta y \end{bmatrix} \end{cases} = \begin{cases} \dot{\hat{x}} = a_K(\hat{x}) + B_K(\hat{x}) \begin{bmatrix} u \\ y \end{bmatrix} \\ r_y = c_K(\hat{x}) + D_K(\hat{x}) \begin{bmatrix} u \\ y \end{bmatrix}, \end{cases} \quad (83)$$

is called *uncertainty model of the SKR* with Δz denoting the uncertainties corrupted in the data (u, y) .

The uncertainty model (82) and the condition (83) imply that,

- on the one hand, the residual vector r_y exclusively contains the information about uncertainties in the system,
- on the other hand, r_y can be equivalently generated by the SKR (16) driven by (u, y) .

Although Δz is in general unknown, its value can be specified in two (extreme) cases, which play an essential role in our subsequent study:

- corresponding to the nominal dynamics,

$$\forall \begin{bmatrix} u \\ y \end{bmatrix} \in \mathcal{I}_\Sigma, \begin{bmatrix} \Delta u \\ \Delta y \end{bmatrix} = 0; \quad (84)$$

- when it holds

$$\begin{aligned}\hat{z}_\Delta &= (D\Sigma_{\mathcal{K}})^T \circ \Sigma_{\mathcal{K}} \left(\begin{bmatrix} u \\ y \end{bmatrix} \right) = (D\Sigma_{\mathcal{K}})^T \circ \Sigma_{\mathcal{K}} \left(\begin{bmatrix} \Delta u \\ \Delta y \end{bmatrix} \right) \\ &= \begin{bmatrix} u \\ y \end{bmatrix} = \begin{bmatrix} \Delta u \\ \Delta y \end{bmatrix}.\end{aligned}\quad (85)$$

The first case is true due to the relation (17) and reflects the system response during nominal operations. The second one means, the data (u, y) solely contains uncertainties, which, despite being rarely the case in real operations, characterises a crucial data set, and induces us to introduce the concept of manifold of uncertain data.

Definition 7 *Given the normalised SKR (16), manifold $\mathcal{U}_\Sigma \subset \mathcal{L}_2$,*

$$\mathcal{U}_\Sigma = \left\{ \begin{bmatrix} u \\ y \end{bmatrix}, \begin{bmatrix} u \\ y \end{bmatrix} = (D\Sigma_{\mathcal{K}})^T (r), r \in \mathcal{L}_2 \right\}, \quad (86)$$

is called manifold of uncertain data.

It is apparent that $\forall \begin{bmatrix} u \\ y \end{bmatrix} \in \mathcal{U}_\Sigma$,

$$\hat{z}_\Delta = (D\Sigma_{\mathcal{K}})^T \circ \Sigma_{\mathcal{K}} \left(\begin{bmatrix} u \\ y \end{bmatrix} \right) = \begin{bmatrix} u \\ y \end{bmatrix},$$

i.e. the relation (85) holds. Thus, the data in \mathcal{U}_Σ solely contain uncertainties. Note that

$$\forall \begin{bmatrix} u \\ y \end{bmatrix} \in \mathcal{L}_2, \begin{bmatrix} \Delta \hat{u} \\ \Delta \hat{y} \end{bmatrix} = (D\Sigma_{\mathcal{K}})^T \circ \Sigma_{\mathcal{K}} \left(\begin{bmatrix} u \\ y \end{bmatrix} \right) \in \mathcal{U}_\Sigma \quad (87)$$

indicates that the operator $(D\Sigma_{\mathcal{K}})^T \circ \Sigma_{\mathcal{K}}$ projects the data (u, y) to the manifold \mathcal{U}_Σ . Observe that, as a result of the uncertainty model (82),

$$\begin{bmatrix} \hat{u}_\Delta \\ \hat{y}_\Delta \end{bmatrix} = (D\Sigma_{\mathcal{K}})^T \circ \Sigma_{\mathcal{K}} \left(\begin{bmatrix} u \\ y \end{bmatrix} \right) = (D\Sigma_{\mathcal{K}})^T \circ \Sigma_{\mathcal{K}} \left(\begin{bmatrix} \Delta u \\ \Delta y \end{bmatrix} \right). \quad (88)$$

That is, $\begin{bmatrix} \hat{u}_\Delta \\ \hat{y}_\Delta \end{bmatrix}$ is a projection of the uncertainty $\begin{bmatrix} \Delta u \\ \Delta y \end{bmatrix}$ corrupted in the system data and thus serves as an estimate of $\begin{bmatrix} \Delta u \\ \Delta y \end{bmatrix}$ in the context of the uncertainty model (82). It can be, for instance, applied for re-constructing the detected faults or examining the data quality. To this end, we will study the normalised SKR and the associated Hamiltonian projection system,

$$\hat{z}_\Delta = \begin{bmatrix} \hat{u}_\Delta \\ \hat{y}_\Delta \end{bmatrix} = (D\Sigma_{\mathcal{K}})^T \circ \Sigma_{\mathcal{K}} \left(\begin{bmatrix} u \\ y \end{bmatrix} \right), \quad (89)$$

in the next subsection.

Remark 4 *We would like to emphasise that \hat{z}_Δ is an estimation of the uncertainty $\begin{bmatrix} \Delta u \\ \Delta y \end{bmatrix}$ corrupted in the system data. And the Hamiltonian projection system (89) is a projection of the data (u, y) onto the manifold of uncertain data \mathcal{U}_Σ .*

4.2 Normalised SKR and the associated Hamiltonian projection system

We begin with the state space description of system (89). Let

$$H(\hat{x}, \lambda, z) = \frac{1}{2} (c_K(\hat{x}) + D_K(\hat{x})z)^T (c_K(\hat{x}) + D_K(\hat{x})z) + \lambda^T (a_K(\hat{x}) + B_K(\hat{x})z) \quad (90)$$

be the Hamiltonian function, where, for the sake of simplicity, notation \hat{x} instead of \hat{x}_Δ is abused. Accordingly, we have

$$(D\Sigma_{\mathcal{K}})^T \circ \Sigma_{\mathcal{K}} : \begin{cases} \dot{\hat{x}} = \frac{\partial H(\hat{x}, \lambda, z)}{\partial \lambda} \\ \dot{\lambda} = -\frac{\partial H(\hat{x}, \lambda, z)}{\partial \hat{x}} \\ \dot{\hat{z}}_\Delta = \frac{\partial H(\hat{x}, \lambda, z)}{\partial z}. \end{cases} \quad (91)$$

By some routine calculations, the Hamiltonian function (90) is further written into

$$\begin{aligned} H(\hat{x}, \lambda, z) &= \frac{1}{2} r_y^T r_y + \lambda^T \dot{\hat{x}} \\ &= \hat{z}_\Delta^T \hat{z}_\Delta + \frac{1}{2} c_K^T(\hat{x}) c_K(\hat{x}) - \frac{1}{2} z^T D_K^T(\hat{x}) D_K(\hat{x}) z + \lambda^T a_K(\hat{x}) \\ &= \hat{z}_\Delta^T z - \frac{1}{2} \hat{z}_\Delta^T \hat{z}_\Delta + c_K^T(\hat{x}) c_K(\hat{x}) + \lambda^T B_K(\hat{x}) D_K^T(\hat{x}) c_K(\hat{x}) \\ &\quad + \frac{1}{2} \lambda^T B_K(\hat{x}) B_K^T(\hat{x}) \lambda + \lambda^T a_K(\hat{x}). \end{aligned} \quad (92)$$

The calculation of the last equation follows from the relations

$$D_K(\hat{x}) D_K^T(\hat{x}) = I, D_K^T(\hat{x}) D_K(\hat{x}) D_K^T(\hat{x}) D_K(\hat{x}) = D_K^T(\hat{x}) D_K(\hat{x}),$$

which are true by setting $W(\hat{x}) = (I + D(\hat{x}) D^T(\hat{x}))^{-1/2}$ and are assumed in our subsequent study. The following theorem gives the Hamiltonian functions $H(\hat{x}, \lambda, z)$ and $H^\times(\hat{x}, \lambda, \hat{z}_\Delta)$ corresponding to the normalised SKR.

Theorem 8 *Given the normalised SKR (16) and the corresponding Hamiltonian system (91), then*

$$H(\hat{x}, \lambda, z) = \hat{z}_\Delta^T z - \frac{1}{2} \hat{z}_\Delta^T \hat{z}_\Delta, \quad (93)$$

$$H^\times(\hat{x}, \lambda, \hat{z}_\Delta) = \frac{1}{2} \hat{z}_\Delta^T \hat{z}_\Delta. \quad (94)$$

Proof. It follows from Lemma 1 and Theorem 1 that for $\lambda = V_{\hat{x}}(\hat{x})$ with $V(\hat{x})$ solving (37)

$$\begin{aligned} c_K^T(\hat{x}) c_K(\hat{x}) + V_{\hat{x}}(\hat{x}) B_K(\hat{x}) D_K^T(\hat{x}) c_K(\hat{x}) &= 0, \\ V_{\hat{x}}^T(\hat{x}) a_K(\hat{x}) + \frac{1}{2} V_{\hat{x}}^T(\hat{x}) B_K(\hat{x}) B_K^T(\hat{x}) V_{\hat{x}}(\hat{x}) &= 0 \\ \implies H^\times(\hat{x}, \lambda, \hat{z}_\Delta) = \frac{1}{2} \hat{z}_\Delta^T \hat{z}_\Delta, H(\hat{x}, \lambda, z) = \hat{z}_\Delta^T z - H^\times(\hat{x}, \lambda, \hat{z}_\Delta) &= \hat{z}_\Delta^T z - \frac{1}{2} \hat{z}_\Delta^T \hat{z}_\Delta. \end{aligned}$$

■

For our study, we are interested in the Hamiltonian functions corresponding to the two extreme cases: (i) $z \in \mathcal{I}_\Sigma$, (ii) $\forall z \in \mathcal{U}_\Sigma$. The following corollary gives the solutions.

Corollary 2 *Given the normalised SKR (16) and the corresponding Hamiltonian system (91), then*

$$\forall z = \begin{bmatrix} u \\ y \end{bmatrix} \in \mathcal{I}_\Sigma, H^\times(x, \lambda, \hat{z}_\Delta) = H(x, \lambda, z) = 0, \quad (95)$$

$$\forall z = \begin{bmatrix} u \\ y \end{bmatrix} \in \mathcal{U}_\Sigma, H(\hat{x}, \lambda, z) = H^\times(\hat{x}, \lambda, \hat{z}_\Delta) = \frac{1}{2} \hat{z}_\Delta^T \hat{z}_\Delta = \frac{1}{2} z^T z. \quad (96)$$

Proof. It follows from (17) (and (84)) that

$$\forall z = \begin{bmatrix} u \\ y \end{bmatrix} \in \mathcal{I}_\Sigma, \begin{bmatrix} \Delta u \\ \Delta y \end{bmatrix} = 0, r_y = 0 \implies \hat{z}_\Delta = 0.$$

Hence, according to Theorem 8,

$$H^\times(x, \lambda, \hat{z}_\Delta) = H(x, \lambda, z) = 0.$$

By Definition 7,

$$\forall z \in \mathcal{U}_\Sigma, \hat{z}_\Delta = (D\Sigma_{\mathcal{K}})^T \circ \Sigma_{\mathcal{K}}(z) = (D\Sigma_{\mathcal{K}})^T \circ \Sigma_{\mathcal{K}}(\Delta z) = z = \Delta z.$$

Thus, it follows from Theorem 8 that

$$H(\hat{x}, \lambda, z) = H^\times(\hat{x}, \lambda, \hat{z}_\Delta) = \frac{1}{2} \hat{z}_\Delta^T \hat{z}_\Delta = \frac{1}{2} z^T z.$$

■

Corollary 2 describes two special operation situations, in which

$$H^\times(x, \lambda, \hat{z}_\Delta) = H(x, \lambda, z).$$

The first one given by (95) corresponds to the nominal dynamics, while the second one with (96) reflects the situation, when the data exclusively consist of uncertainties.

4.3 Applications to fault detection and uncertainty estimation

Based on the results presented in the previous subsections, Bregman divergence-based fault detection schemes as well as a further study on uncertainty estimation are addressed in this subsection.

4.3.1 Bregman divergence-based fault detection

To begin with, we discuss about the application of the Bregman divergence from the estimated uncertainty in the data, \hat{z}_Δ , to the manifold \mathcal{I}_Σ for the purpose of fault detection. Consider the uncertainty model (82) and recall that

$$\forall \begin{bmatrix} u \\ y \end{bmatrix} \in \mathcal{I}_\Sigma, \begin{bmatrix} \Delta u \\ \Delta y \end{bmatrix} = \begin{bmatrix} \hat{u}_\Delta \\ \hat{y}_\Delta \end{bmatrix} = 0. \quad (97)$$

To detect possible uncertainties in the data (u, y) , the Hamiltonian function

$$H^\times(\hat{z}_\Delta) := H^\times(\hat{x}, \lambda, \hat{z}_\Delta) = \frac{1}{2} \hat{z}_\Delta^T \hat{z}_\Delta$$

can be used. Note that the Bregman divergence from \hat{z}_Δ to the manifold \mathcal{I}_Σ derived from $H^\times(\hat{z}_\Delta)$ is given by, due to (97),

$$D_{H^\times}[\hat{z}_\Delta : 0] = H^\times(\hat{z}_\Delta) = \frac{1}{2}\hat{z}_\Delta^T \hat{z}_\Delta. \quad (98)$$

It is of interest to notice that the Bregman divergence (98) is true for all (u, y) belonging to \mathcal{I}_Σ . Moreover, $\hat{z}_\Delta = (D\Sigma_{\mathcal{K}})^T \circ \Sigma_{\mathcal{K}}(z)$. In this sense, $D_{H^\times}[\hat{z}_\Delta : 0]$ can be interpreted as a divergence from the uncertainty in the data to \mathcal{I}_Σ .

Analogue to the discussion on the implementation issues in Subsection 3.3, we shortly summarise the major steps to apply the Bregman divergence (98) for a practical fault detection. Let $z(k_i), i = 1, \dots, M$, be the data collected over the time interval $[t_0, t_1]$ and

$$J = \frac{1}{M} \sum_{i=1}^M D_{H^\times}[\hat{z}_\Delta(k_i) : 0] = \frac{1}{2M} \sum_{i=1}^M \hat{z}_\Delta^T(k_i) \hat{z}_\Delta(k_i) = \frac{1}{2} \hat{z}_{\Delta M}^T \hat{z}_{\Delta M}, \quad (99)$$

$$\hat{z}_{\Delta M} = \begin{bmatrix} \frac{\hat{z}_\Delta(k_1)}{\sqrt{M}} \\ \vdots \\ \frac{\hat{z}_\Delta(k_M)}{\sqrt{M}} \end{bmatrix} \in \mathbb{R}^{M(m+p)}, z_M = \begin{bmatrix} \frac{z(k_1)}{\sqrt{M}} \\ \vdots \\ \frac{z(k_M)}{\sqrt{M}} \end{bmatrix} \in \mathbb{R}^{M(m+p)},$$

be the corresponding evaluation function. It is straightforward that the evaluation function (99) is a Bregman divergence with the generating function $\frac{1}{2}\hat{z}_{\Delta M}^T \hat{z}_{\Delta M}$, namely

$$J = D_{H^\times}[z_M : 0] = \frac{1}{2}\hat{z}_{\Delta M}^T \hat{z}_{\Delta M}.$$

To set the threshold, consider the ratio

$$\frac{\hat{z}_{\Delta M}^T \hat{z}_{\Delta M}}{z_M^T z_M}$$

that gives an estimate of the relative change in the process data z_M . Let $\alpha \in (0, 1)$ be the tolerant limit so that it is accepted as fault-free operation when

$$\frac{\hat{z}_{\Delta M}^T \hat{z}_{\Delta M}}{z_M^T z_M} \leq \alpha.$$

Accordingly, the threshold is set to be

$$J_{th} = \frac{\alpha}{2} z_M^T z_M. \quad (100)$$

Below is the online detection algorithm:

- Collection of data $z(k_i)$ and computation of $\hat{z}(k_i), i = 1, \dots, M$, according to (78);
- Computation of the evaluation function J according to (99);
- Detection decision logic:

$$\begin{cases} J \leq J_{th} \implies \text{fault-free} \\ J > J_{th} \implies \text{faulty.} \end{cases}$$

4.3.2 On the projection-based estimation

Having studied the use of the projection, $\hat{z}_\Delta = (D\Sigma_{\mathcal{K}})^T (r_y) = (D\Sigma_{\mathcal{K}})^T \circ \Sigma_{\mathcal{K}}(z)$, for the fault detection purpose, we now comprehend \hat{z}_Δ as an estimate of uncertainties corrupted in the data. To this end, two issues are addressed: (i) examining \hat{z}_Δ as a projection of the system data on the uncertain data manifold \mathcal{U}_Σ , from the viewpoint of information geometry, and (ii) considering \hat{z}_Δ as an estimate of Δz subject to the uncertainty model (82) and examining the corresponding residual r_y .

The following theorem is a dual result of Theorem 6 and gives \hat{z}_Δ an insightful interpretation from the information geometric viewpoint.

Theorem 9 Consider the normalised SKR (16) and the Bregman divergence $D_{H^\times} [z : \mathcal{U}_\Sigma]$,

$$\begin{aligned} D_{H^\times} [z : \mathcal{U}_\Sigma] &= \min_{\Delta z_0 \in \mathcal{U}_\Sigma} D_{H^\times} [z : \Delta z_0], \\ D_{H^\times} [z : \Delta z_0] &:= H^\times(z) - H^\times(\Delta z_0) - \left(\frac{\partial H^\times(\Delta z_0)}{\partial \Delta z_0} \right)^T (z - \Delta z_0), \\ H^\times(z) &= \hat{z}_\Delta^T z - H(\hat{x}, \lambda, z) = \frac{1}{2} \hat{z}_\Delta^T \hat{z}_\Delta. \end{aligned}$$

The projection \hat{z}_Δ delivered by the corresponding Hamiltonian system (91) is a geodesic projection of z onto \mathcal{U}_Σ .

Proof. The proof is similar to the one of Theorem 6. Thus, only key steps are described. According to Theorem 2, the geodesic projection of z onto \mathcal{U}_Σ is the vector Δz^* leading to

$$\min_{\Delta z_0 \in \mathcal{U}_\Sigma} D_{H^\times} [z : \Delta z_0] = D_{H^\times} [z : \Delta z^*].$$

Following (40) and noticing

$$\forall \Delta z_0 \in \mathcal{U}_\Sigma, \Delta z_0^\times = \hat{z}_{\Delta 0} = (D\Sigma_{\mathcal{K}})^T \circ \Sigma_{\mathcal{K}}(\Delta z_0) = \Delta z_0,$$

it turns out

$$D_{H^\times} [z : \Delta z_0] = H^\times(z) + H(\Delta z_0^\times) - z^T \Delta z_0^\times = H^\times(z) + H(\Delta z_0) - z^T \Delta z_0.$$

It yields, by Theorem 8 and Corollary 2,

$$H(\Delta z_0) = \frac{1}{2} \Delta z_0^T \Delta z_0 \implies D_{H^\times} [z : \Delta z_0] = H^\times(z) + \frac{1}{2} \Delta z_0^T \Delta z_0 - z^T \Delta z_0,$$

which leads to

$$\min_{\Delta z_0 \in \mathcal{U}_\Sigma} D_{H^\times} [z : \Delta z_0] \iff \min_{\Delta z_0 \in \mathcal{U}_\Sigma} \left(\frac{1}{2} \Delta z_0^T \Delta z_0 - z^T \Delta z_0 \right).$$

Since $\forall \Delta z_0 \in \mathcal{U}_\Sigma$,

$$\begin{aligned} \Delta z_0 &= B_K^T(\hat{x})V_{\hat{x}}(\hat{x}) + D_K^T(\hat{x})c_K(\hat{x}) + D_K^T(\hat{x})D_K(\hat{x})\Delta z_0, \\ D_K(\hat{x})D_K^T(\hat{x}) &= I, (B_K^T(\hat{x})V_{\hat{x}}(\hat{x}) + D_K^T(\hat{x})c_K(\hat{x}))^T D_K^T(\hat{x}) = 0, \end{aligned}$$

it holds

$$\begin{aligned}
\Delta z_0^T \Delta z_0 &= \Delta z_0^T D_K^T(\hat{x}) D_K(\hat{x}) \Delta z_0 \\
&+ (B_K^T(\hat{x}) V_{\hat{x}}(\hat{x}) + D_K^T(\hat{x}) c_K(\hat{x}))^T (B_K^T(\hat{x}) V_{\hat{x}}(\hat{x}) + D_K^T(\hat{x}) c_K(\hat{x})), \\
z^T \Delta z_0 &= z^T (B_K^T(\hat{x}) V_{\hat{x}}(\hat{x}) + D_K^T(\hat{x}) c_K(\hat{x}) + D_K^T(\hat{x}) D_K(\hat{x}) \Delta z_0) \implies \\
&\min_{\Delta z_0 \in \mathcal{U}_\Sigma} \left(\frac{1}{2} \Delta z_0^T \Delta z_0 - z^T \Delta z_0 \right) \iff \\
&\min_{\Delta z_0 \in \mathcal{U}_\Sigma} \left(\frac{1}{2} \Delta z_0^T D_K^T(\hat{x}) D_K(\hat{x}) \Delta z_0 - z^T D_K^T(\hat{x}) D_K(\hat{x}) \Delta z_0 \right).
\end{aligned}$$

Solving

$$\frac{\partial}{\partial \Delta z_0} \left(\frac{1}{2} \Delta z_0^T D_K^T(\hat{x}) D_K(\hat{x}) \Delta z_0 - z^T D_K^T(\hat{x}) D_K(\hat{x}) \Delta z_0 \right) = 0$$

gives

$$D_K^T(\hat{x}) D_K(\hat{x}) \Delta z^* = D_K^T(\hat{x}) D_K(\hat{x}) z \tag{101}$$

where Δz^* represents the optimal solution belonging to \mathcal{U}_Σ . It is obvious that

$$\hat{z}_\Delta = B_K^T(\hat{x}) V_{\hat{x}}(\hat{x}) + D_K^T(\hat{x}) c_K(\hat{x}) + D_K^T(\hat{x}) D_K(\hat{x}) z \in \mathcal{U}_\Sigma$$

solves (101), which proves $\Delta z^* = \hat{z}_\Delta$. ■

Theorem 9 underlines \hat{z}_Δ as an optimal estimate for Δz in the context of a geodesic projection of z onto \mathcal{U}_Σ . Here, the manifold \mathcal{U}_Σ is equipped with a dual Riemannian structure by means of the Bregman divergence D_{H^\times} and it is dually flat (Amari, 2016).

Next, consider the SKR (16) and the estimator

$$\hat{z}_\Delta = \begin{bmatrix} \hat{u}_\Delta \\ \hat{y}_\Delta \end{bmatrix} = (D\Sigma_{\mathcal{K}})^T (r_y), \tag{102}$$

$$(D\Sigma_{\mathcal{K}})^T : \begin{cases} \dot{\lambda} = - \left(\frac{\partial a_K(\hat{x})}{\partial \hat{x}} + \frac{\partial B_K(\hat{x})}{\partial \hat{x}} z \right)^T \lambda - \left(\frac{\partial c_K(\hat{x})}{\partial \hat{x}} + \frac{\partial D_K(\hat{x})}{\partial \hat{x}} \right)^T r_y \\ \begin{bmatrix} \hat{u}_\Delta \\ \hat{y}_\Delta \end{bmatrix} = B_K^T(\hat{x}) \lambda + D_K^T(\hat{x}) r_y. \end{cases} \tag{103}$$

To guarantee that the delivered estimate \hat{z}_Δ is subject to the uncertainty model (82), it is required that

$$\Sigma_{\mathcal{K}} \left(\begin{bmatrix} \hat{u}_\Delta \\ \hat{y}_\Delta \end{bmatrix} \right) = r_y \implies r_y = \Sigma_{\mathcal{K}} \circ (D\Sigma_{\mathcal{K}})^T (r_y). \tag{104}$$

It is apparent that the normalised SKR, as a co-inner, satisfies the condition (104). Below, it is delineated that a normalised SKR based estimator (102) delivers an LS estimation in the context that it solves the optimisation problem

$$\begin{aligned}
&\min_{L(\hat{x})} \frac{1}{2} \int_0^\infty r_y^T r_y dt \\
&\text{s.t. } \dot{\hat{x}} = a_K(\hat{x}) + B_K(\hat{x}) \hat{z}_\Delta.
\end{aligned} \tag{105}$$

To this end, an arbitrary SKR with

$$W(\hat{x}) = (I + D(\hat{x})D^T(\hat{x}))^{-1/2} \implies D_K(\hat{x})D_K^T(\hat{x}) = I$$

is considered.

Observe that the condition (104) implies

$$r_y = c_K(\hat{x}) + D_K(\hat{x})B_K^T(\hat{x})\lambda + r_y \iff c_K(\hat{x}) + D_K(\hat{x})B_K^T(\hat{x})\lambda = 0.$$

Moreover, it holds

$$\begin{aligned} & \frac{1}{2}r_y^T r_y + \lambda^T (a_K(\hat{x}) + B_K(\hat{x})B_K^T(\hat{x})\lambda + B_K(\hat{x})D_K^T(\hat{x})r_y) \\ &= \frac{1}{2} (B_K^T(\hat{x})\lambda + D_K^T(\hat{x})r_y)^T (B_K^T(\hat{x})\lambda + D_K^T(\hat{x})r_y) + \lambda^T \left(a_K(\hat{x}) + \frac{1}{2}B_K(\hat{x})B_K^T(\hat{x})\lambda \right) \\ &= \frac{1}{2}\hat{z}_\Delta^T \hat{z}_\Delta + \lambda^T \left(a_K(\hat{x}) + \frac{1}{2}B_K(\hat{x})B_K^T(\hat{x})\lambda \right). \end{aligned}$$

Now, let

$$\begin{aligned} \bar{H}(\hat{x}, \lambda, \hat{z}_\Delta) &:= \frac{1}{2}\hat{z}_\Delta^T \hat{z}_\Delta + \lambda^T \left(a_K(\hat{x}) + \frac{1}{2}B_K(\hat{x})B_K^T(\hat{x})\lambda \right) \\ &= \frac{1}{2}r_y^T r_y + \lambda^T (a_K(\hat{x}) + B_K(\hat{x})\hat{z}_\Delta), \end{aligned}$$

and calculate

$$\frac{\partial}{\partial L(\hat{x})} \bar{H}(\hat{x}, \lambda, \hat{z}_\Delta) = \frac{\partial}{\partial L(\hat{x})} \left(\begin{array}{c} \frac{1}{2}\lambda^T L(\hat{x}) (I + D(\hat{x})D^T(\hat{x})) L^T(\hat{x})\lambda \\ -\lambda^T L(\hat{x}) (c(\hat{x}) + D(\hat{x})B^T(\hat{x})\lambda) \end{array} \right).$$

It is apparent that λ and $L^*(\hat{x})$ adopted in the normalised SKR and satisfying (37)-(38) solve the equation

$$\frac{\partial}{\partial L(\hat{x})} \bar{H}(\hat{x}, \lambda, \hat{z}_\Delta) = 0.$$

As a result, we obtain

$$L^*(\hat{x}) = \arg \min_{L(\hat{x})} \bar{H}(\hat{x}, \lambda, \hat{z}_\Delta). \quad (106)$$

It is well-known from the calculus of variations that

$$\bar{H}(\hat{x}, \lambda, \hat{z}_\Delta) = \frac{1}{2}r_y^T r_y + \lambda^T (a_K(\hat{x}) + B_K(\hat{x})\hat{z}_\Delta)$$

can be interpreted as the Hamiltonian function of the optimisation problem (105), and the optimal solution given by solving (106). In this regard, the uncertainty estimate \hat{z}_Δ delivered by the estimator (102) is an LS estimate subject to the uncertainty model (82) with r_y as its output whose \mathcal{L}_2 -norm is at a minimum.

5 Conclusions

In this draft, performance-oriented one-class fault detection and estimation in nonlinear dynamic systems with uncertainties have been addressed. Bearing in mind that the objective of this work is to establish a framework, in which not only model-based but also data-driven and ML-based fault diagnosis strategies can be uniformly handled, our work has followed a paradigm that is different from the conventional control theoretically oriented model-based framework. To be specific, our work is based on the SIR and SKR model forms of dynamic systems, rather than on the well-established input-output and the associated state space models. This change enables us to model the nominal system dynamics as a lower-dimensional manifold embedded in the process data space (u, y) . The main idea behind this handling is, along the line of data-driven and ML-based fault detection schemes, to deal with fault detection as a classification problem in the process data space. To this end, projection technique provides us with a capable mathematical tool. In this regard, our work has focused on projection-based fault detection and estimation in nonlinear dynamic systems.

Encouraged by our previous work on application of the orthogonal projection technique to fault detection in LTI systems (Ding *et al.*, 2022), we have started our effort with constructing projection systems. As an extension of the well-established projections onto the image and kernel subspaces of LTI systems (Georgiou, 1988; Vinnicombe, 2000; Ding *et al.*, 2022), normalised SIR and SKR of nonlinear systems have been adopted for our purpose. In order to address nonlinear system specified issues, we have focused on the lossless properties of the normalised SIR and SKR as inner and co-inner, and introduced various configurations of Hamiltonian extensions (Crouch and van der Schaft, 1987) as Hamiltonian systems (Scherpen and van der Schaft, 1994; Ball and van der Schaft, 1996; Petersen and der Schaft, 2005). They serve as the system theoretical tool throughout our work.

The theoretical basis for a successful application of the orthogonal projection technique to fault detection in LTI systems is the Pythagorean Theorem. Concretely, the normalised SIR-based orthogonal projection of the process data (u, y) onto the image subspace in Hilbert space, describing the nominal system dynamics, allows an orthogonal decomposition of (u, y) into an optimal estimate (projection) and the residual. By means of the Pythagorean equation, a norm-based evaluation of (u, y) leads to a unique separation of the nominal dynamic and the dynamics corresponding to uncertainties/faults. As a result, a classification and thus an optimal fault detection is achieved. For nonlinear dynamic systems, (process) data processing should be performed in non-Euclidean space. Consequently, the norm-based distance defined in Hilbert space may not be compatible with the metric tensor of the non-Euclidean space and hence is not suitable to measure the distance from a data vector to the system image manifold. As one of the major contributions of our work, we have proposed to use a Bregman divergence, a measure of difference between two points in a space, to solve this problem. A Bregman divergence is defined in terms of a convex function. When the system performance function under consideration is convex, it is plain that we are able to use the Bregman divergence defined by such a performance to achieve performance-oriented fault detection. A further distinguishing contribution of our work is the proposed scheme of combining the normalised SIR as Hamiltonian systems and the Bregman divergence induced by the corresponding Hamiltonian functions. This scheme not only enables to realise the objective of performance-oriented fault detection, but also uncovers the information geometric aspect of our work. It is known that the input and output of a Hamiltonian system build

a Legendre transform and there exists a Hamiltonian system as the Legendre dual system. As a result, the computation of the corresponding Bregman divergence can be expressed in terms of the dual Hamiltonian functions. In particular, a Bregman divergence together with a Legendre transform may induce a dually flat Riemannian manifold in the data space that may be regarded as a dualistic extension of the Euclidean space (Amari, 2016; Nielsen, 2020). In this context, the Hamiltonian system based projection can be interpreted as a geodesic projection. So far, this part of work is an integration of control theory and information geometry, whose main results are summarised as follows:

- Construction of the normalised SIR-based projection system that projects (u, y) onto \mathcal{I}_Σ , the image manifold describing the nominal system dynamics,
- Determination of the Hamiltonian functions with respect to the nominal dynamics,
- Determination and computation of the Bregman divergence for performance-oriented fault detection, and based on it,
- Definition of the evaluation function over a time interval, which has been proved to be a Bregman divergence as well, and the corresponding threshold setting,
- Demonstration of the interpretation that the projection onto the image manifold is a geodesic projection.

As reported in our previous work (Ding *et al.*, 2022), for LTI systems the orthogonal projection onto the image subspace is equivalent to a projection onto the kernel subspace. Thanks to the Pythagorean equation, the projection-based fault detection can then be equivalently realised using an observer-based residual generator. These conclusions and results have motivated and inspired our study on the normalised SKR induced Hamiltonian system $(D\Sigma_{\mathcal{K}})^T \circ \Sigma_{\mathcal{K}}$ as a projection. Since the SKR $\Sigma_{\mathcal{K}}$ is a residual generator and the residual contains uncertainty information, we have firstly studied $(D\Sigma_{\mathcal{K}})^T \circ \Sigma_{\mathcal{K}}$ and its co-inner property from the information (uncertainty) viewpoint. To be specific, the uncertainty model (82) and Definition 7, the manifold of uncertain data \mathcal{U}_Σ , have been introduced. It has been proved that $(D\Sigma_{\mathcal{K}})^T \circ \Sigma_{\mathcal{K}}$ represents a projection of the process data onto \mathcal{U}_Σ . Analogue to our work in the first part, a fault detection scheme has been proposed, consisting of

- design of $(D\Sigma_{\mathcal{K}})^T \circ \Sigma_{\mathcal{K}}$ and the corresponding dual Hamiltonian system,
- determination of the Hamiltonian functions with respect to the two extreme cases, $z \in \mathcal{I}_\Sigma$ and $z \in \mathcal{U}_\Sigma$,
- definition and computation of the Hamiltonian function induced Bregman divergence and its use for fault detection,
- analysis and interpretation of $(D\Sigma_{\mathcal{K}})^T \circ \Sigma_{\mathcal{K}}$ as a projection onto \mathcal{U}_Σ , and
- study on the realisation issues.

The further contribution of our study on $(D\Sigma_{\mathcal{K}})^T \circ \Sigma_{\mathcal{K}}$ is the proof that the projection is an LS estimation of the uncertainty corrupted in (u, y) and subject to the uncertainty model. An immediate application of this result is fault estimation. In other words, variations in the

process data caused by faults, in particular those process faults, are modelled like uncertainties by means of the uncertainty model and the manifold \mathcal{U}_Σ represents the corresponding set in the data space. And $(D\Sigma_{\mathcal{K}})^T \circ \Sigma_{\mathcal{K}}$ serves as an optimal (LS) estimator for such variations in the process data.

Our future work will concentrate on two aspects aiming at the overall goal of our efforts to build a uniform framework. The first one is the work on an ML-based realisation of the Hamiltonian projection systems. In this work, we will focus on AE learning methods. In fact, both projection systems studied in this draft, $\Sigma_{\mathcal{I}} \circ (D\Sigma_{\mathcal{I}})^T$ and $(D\Sigma_{\mathcal{K}})^T \circ \Sigma_{\mathcal{K}}$, are of the typical configuration of an AE, where the latent variables are v and r_y respectively. In our previous work (Li *et al.*, 2022), we have proposed to train $\Sigma_{\mathcal{I}} \circ (D\Sigma_{\mathcal{I}})^T$ as neural networks (NNs) in such a way that $\Sigma_{\mathcal{I}} \circ (D\Sigma_{\mathcal{I}})^T$ is idempotent and of the lossless property. In our future work, the corresponding Bregman divergences and Legendre transform will be integrated into the learning process, and $(D\Sigma_{\mathcal{K}})^T \circ \Sigma_{\mathcal{K}}$ will be considered as well. This work can be interpreted as control theoretically learning of AE for optimal and data-driven fault diagnosis. The second aspect is the application of PINN methods (Karniadakis *et al.*, 2021). In our theoretical work, we notice that solving HJEs like (34) and (37) analytically is a hard work. The PINN methods offer a capable tool to deal with such problems.

Acknowledgement: The authors are very grateful to Prof. Y. Yang for the collaborative and valuable support.

References

- Adamcik, M. (2014). The information geometry of bregman divergences and some applications in multi-expert reasoning. *Entropy* **16**(12), 6338–6381.
- Ahmed, I., T. Galoppo, X. Hu and Y. Ding (2022). Graph regularized autoencoder and its application in unsupervised anomaly detection. *IEEE Transactions on Pattern Analysis and Machine Intelligence* **44**(8), 4110–4124.
- Alcorta-Garcia, E. and P.M. Frank (1997). Deterministic nonlinear observer based approaches to fault diagnosis: A survey. *Control Engineering practice* **5**(5), 663–670.
- Amari, S. (2016). *Information Geometry and its Applications*. Springer. Japan.
- Armeni, A., A. Casavola and E. Mosca (2009). Robust fault detection and isolation for LPV systems under a sensitivity constraint. *Int. J. Adapt. Control and Signal process.* **23**, 55–72.
- Ball, J. A. and A. J. van der Schaft (1996). J-inner-outer factorization, j-spectral factorization, and robust control for nonlinear systems. *IEEE Trans. on Automatic Contr.* **41**, 379–392.
- Blanke, M., M. Kinnaert, J. Lunze and M. Staroswiecki (2006). *Diagnosis and Fault-Tolerant Control, 2nd Edition*. Springer. Berlin Heidelberg.
- Bokor, J. and G. Balas (2004). Detection filter design for LPV systems - a geometric approach. *Automatica* **40**, 511–518.

- Bregman, L.M. (1967). The relaxation method of finding the common point of convex sets and its application to the solution of problems in convex programming. *USSR Computational Mathematics and Mathematical Physics* **7**(3), 200–217.
- Chadli, M., A. Abdo and S. X. Ding (2013). h_-/h_{inf} fault detection filter design for discrete-time takagi-sugeno fuzzy system. *Automatica* **49**, 1996–2005.
- Chen, J. and R. J. Patton (1999). *Robust Model-Based Fault Diagnosis for Dynamic Systems*. Kluwer Academic Publishers. Boston.
- Crouch, P.E. and A.J. van der Schaft (1987). *Variational and Hamiltonian Control Systems*. Springer-Verlag. Basel.
- Ding, S. X. (2008). *Model-Based Fault Diagnosis Techniques - Design Schemes, Algorithms, and Tools*. Springer-Verlag.
- Ding, S. X. (2015). Application of factorization and gap metric techniques to fault detection and isolation part II: Gap metric technique aided FDI performance analysis. In: *Proc. Of IFAC SAFEPROCESS*.
- Ding, S. X. (2020). *Advanced Methods for Fault Diagnosis and Fault-tolerant Control*. Springer-Verlag. Berlin.
- Ding, S. X., L. Li and T. Liu (2022). An alternative paradigm of fault diagnosis in dynamic systems: orthogonal projection-based methods. *arXiv:2202.08108*.
- Feintuch, A. (1998). *Robust Control Theory in Hilbert Space*. Springer-Verlag. New York.
- Floquet, T., J. P. Barbot, W. Perruquetti and M. Djemai (2004). On the robust fault detection via sliding mode disturbance observer. *Int. J. Control* **77**, 622–629.
- Francis, B. A. (1987). *A Course in H-Infinity Control Theory*. Springer-Verlag. Berlin – New York.
- Frank, P. M. (1990). Fault diagnosis in dynamic systems using analytical and knowledge-based redundancy - a survey. *Automatica* **26**, 459–474.
- Frank, P. M. and X. Ding (1997). Survey of robust residual generation and evaluation methods in observer-based fault detection systems. *Journal of Process Control* **7**(6), 403–424.
- Frigyik, B. A., S. Srivastava and M. R. Gupta (2008). Functional bregman divergence and bayesian estimation of distributions. *IEEE Transactions on Information Theory* **54**(11), 5130–5139.
- Gao, Z. W., C. Cecati and S. X. Ding (2015). A survey of fault diagnosis and fault-tolerant techniques, part i: Fault diagnosis with model-based and signal-based approaches. *IEEE Trans. on Industrial Electronics* **62**, 3757–3767.
- Georgiou, T. T (1988). On the computation of the gap metric. *Syst. Contr. Letters* **11**, 253–257.
- Georgiou, T. T and M. C. Smith (1990). Optimal robustness in the gap metric. *IEEE Trans. on Automatic Control* **35**, 673–686.

- Gertler, J. J. (1998). *Fault Detection and Diagnosis in Engineering Systems*. Marcel Dekker. New York Basel Hong Kong.
- Goodfellow, I., Y. Bengio and A. Courville (2016). *Deep Learning*. MIT Press.
- Hammouri, H., M. Kinnaert and E.H. El Yaagoubi (1999). Observer-based approach to fault detection and isolation for nonlinear systems. *IEEE Trans. on Automatic Control* **44**(10), 1879–1884.
- He, X., Z. Wang and D. Zhou (2009). Robust hinf filtering for time-delay systems with probabilistic sensor faults. *IEEE Signal Process. Lett.* **16**, 442–445.
- Hinton, G. E. and R. R. Salakhutdinov (2006). Reducing the dimensionality of data with neural networks. *Science* **313**(5786), 504–507.
- Hoffmann, J. W. (1996). Normalized coprime factorizations in continuous and discrete time - a joint state-space approach. *IMA Journal of Mathematical Control and Information* **13**(4), 359–384.
- Hu, Z., H. Zhao and J. Peng (2022). Low-rank reconstruction-based autoencoder for robust fault detection. *Control Engineering Practice* **123**, 105156.
- Hwang, I., S. Kim, Y. Kim and C. E. Seah (2010). A survey of fault detection, isolation, and reconfiguration methods. *IEEE Trans. Contr. Syst. Tech.* **18**, 636–653.
- Jiang, Li, Zhiqiang Ge and Zhihuan Song (2017). Semi-supervised fault classification based on dynamic sparse stacked auto-encoders model. *Chemometrics and Intelligent Laboratory Systems* **168**, 72–83.
- Kabore, P. and H. Wang (2001). Design of fault diagnosis filters and fault-tolerant control for a class of nonlinear systems. *IEEE Trans. on Autom. Control* **46**, 1805–1810.
- Karniadakis, G.E., I.G. Kevrekidis, L. Lu, P. Perdikaris, S. Wang and L. Yang (2021). Physics-informed machine learning. *Nat Rev Phys* **3**, 422–440.
- Kato, T. (1995). *Perturbation Theory for Linear Operators*. Springer-Verlag. Berlin.
- Li, L. and S. X. Ding (2020). Gap metric techniques and their application to fault detection performance analysis and fault isolation schemes. *Automatica* **118**, 109029.
- Li, L., H. Luo, S. X. Ding, Y. Yang and K. Peng (2019). Performance-based fault detection and fault-tolerant control for automatic control systems. *Automatica* **99**, 389–316.
- Li, L., S. X. Ding, H. Luo, K. Peng and Y. Yang (2020). Performance-based fault-tolerant control approaches for industrial processes with multiplicative faults. *IEEE Trans. on Industrial Informatics* **16**(7), 4759–4768.
- Li, L., S. X. Ding, J. Qui, Y. Yang and D. Xu (2017). Fuzzy observer-based fault detection design approach for nonlinear processes. *IEEE Trans. on Syst., Man, and Cybernetics: Systems* **47**, 1941–1952.

- Li, L., S. X. Ding, J. Qui, Y. Yang and Y. Zhang (2016). Weighted fuzzy observer-based fault detection approach for discrete-time nonlinear systems via piecewise-fuzzy lyapunov functions. *IEEE Trans. on Fuzzy Systems* **24**, 1320–1333.
- Li, L, S. X. Ding, K. Liang, Z. Chen and T. Xue (2022). Control theoretically explainable application of autoencoder methods to fault detection in nonlinear dynamic systems. *arXiv:2208.01921v1*.
- Liu, X., J. Yu and Y. Ye (2021). Residual attention convolutional autoencoder for feature learning and fault detection in nonlinear industrial processes. *Neural Computing & Applications* **33**(19), 12737–12753.
- Lu, W.-M. (1995). A state-space approach to parameterization of stabilizing controllers for nonlinear systems. *IEEE Trans. on Automatic Control* **40**, 1576–1588.
- Mangoubi, R., M. Desai, A. Edelmayer and P. Sammak (2009). Robust detection and estimation in dynamic systems and statistical signal processing: Intersection, parallel paths and applications. *European Journal of Control* **15**, 348–369.
- Nagaoka, H. and S. Amari (1982). Differential geometry of smooth families of probability distributions. Technical Report Technical Report METR 82–7. University of Tokyo.
- Nguang, S. K., P. Shi and S.X. Ding (2007). Fault detection for uncertain fuzzy systems: An LMI approach. *IEEE Trans. on Fuzzy Systems* **15**, 1251–1262.
- Nielsen, Frank (2020). An elementary introduction to information geometry. *Entropy* **22**(10), 1100.
- Patton, R. J., P. M. Frank and R. N. Clark (Ed) (1989). *Fault Diagnosis in Dynamic Systems, Theory and Applications*. Prentice-Hall. Englewood Cliffs, NJ.
- Persis, C. D. and A. Isidori (2001). A geometric approach to nonlinear fault detection and isolation. *IEEE Trans. on Autom. Control* **46**, 853–865.
- Pertew, A. M., H. J. Marquez and Q. Zhao (2007). LMI-based sensor fault diagnosis for nonlinear lipschitz systems. *Automatica* **43**, 1464–1469.
- Petersen, M. A. and A.J. Van der Schaft (2005). Nonsquare spectral factorization for nonlinear control systems. *IEEE Trans. on Autom. Control* **50**, 286–298.
- Ren, Z., W. Zhang and Z. Zhang (2020). A deep nonnegative matrix factorization approach via autoencoder for nonlinear fault detection. *IEEE Trans. Ind. Inform.* **16**(8), 5042–5052.
- Roweis, S. T. and L. K. Saul (2000). Nonlinear dimensionality reduction by locally linear embedding. *Science* **290**, 2323–2326.
- Scherpen, J. M. A. and A.J. van der Schaft (1994). Normalized coprime factorization and balancing for unstable nonlinear systems. *Int. J. Control* **60**, 1193–1222.
- Seliger, R. and P.M. Frank (1991). Fault diagnosis by disturbance decoupled nonlinear observers. In: *Proceedings of the CDC91*. Brighton, England. pp. 2248–2253.

- Shen, Q., B. Jiang and P. Shi (2014). Adaptive fault diagnosis for T–S fuzzy systems with sensor faults and system performance analysis. *IEEE Transactions on Fuzzy Systems* **22**(2), 274–285.
- Sontag, E. D. and Y. Wang (1995). On characterizations of the input-to-state stability property. *Syst. Contr. Lett.* **24**, 351–359.
- Tenenbaum, J. B., V. de Silva and J. C. Langford (2000). A global geometric framework for nonlinear dimensionality reduction. *Science* **290**, 2319–2323.
- van der Schaft, A. (2000). *L2 - Gain and Passivity Techniques in Nonlinear Control*. Springer. London.
- Venkatasubramanian, V., R. Rengaswamy, K. Yin and S.N. Kavuri (2003). A review of process fault detection and diagnosis part I: Quantitative model-based methods. *Computers and Chemical Engineering* **27**, 293–311.
- Vidyasagar, M. (1980). On the stabilization of nonlinear systems using state detection. *IEEE Trans. on Automat. Control* **25**, 504–509.
- Vinnicombe, G. (2000). *Uncertainty and Feedback: H_∞ Loop-Shaping and the ν Gap Metric*. World Scientific.
- Wang, Y., P. He, P. Shi and H. Zhang (2022). Fault detection for systems with model uncertainty and disturbance via coprime factorization and gap metric. *IEEE Transactions on Cybernetics* **52**(8), 7765–7775.
- Xu, A. and Q. Zhang (2004). Nonlinear system fault diagnosis based on adaptive estimation. *Automatica* **40**, 1181–1193.
- Yan, X.-G. and Ch. Edwards (2008). Robust sliding mode observer-based actuator fault detection and isolation for a class of nonlinear systems. *Int. J. Syst. Sci.* **39**, 349–359.
- Yang, Y., S. X. Ding and L. Li (2015). On observer-based fault detection for nonlinear systems. *Syst. Contr. Lett.* **82**, 1399–1410.
- Yang, Y., S. X. Ding and L. Li (2016). Parametrization of nonlinear observer-based fault detection systems. *IEEE Trans. on Automatic Control* **61**, 3687–3692.
- Zhang, X., M. M. Polycarpou and T. Parisini (2010a). Adaptive fault diagnosis and fault-tolerant control of MIMO nonlinear uncertain systems. *Int. J. of Contr.* **83**, 1054–1080.
- Zhang, X., M. M. Polycarpou and T. Parisini (2010b). Fault diagnosis of a class of nonlinear uncertain systems with lipschitz nonlinearities using adaptive estimation. *Automatica* **46**, 290–299.
- Zhong, M. Y., T. Xue and S.X. Ding (2018). A survey on model-based fault diagnosis for linear discrete time varying systems. *Neurocomputing* **306**, 51–60.
- Zhou, K., J.C. Doyle and K. Glover (1996). *Robust and Optimal Control*. Prentice-Hall. Upper Saddle River, New Jersey.